

Organic corrosion inhibitors: where are we now? A review. Part II. Passivation and the role of chemical structure of carboxylates

Yu.I. Kuznetsov

*A.N. Frumkin Institute of Physical Chemistry and Electrochemistry, Russian Academy
of Sciences, Leninskii pr. 31, Moscow, 119071 Russian Federation*

E-mail: kuznetsov@ipc.rssi.ru

Abstract

This article provides an overview of works (2006–2016) devoted to the passivation of various metals and the influence of organic carboxylic acids and their salts thereon. The results of corrosion and electrochemical studies, as well studies on the composition and structural features of surface layers on the metals being protected by a variety of physico-chemical methods are considered.

Key words: *metal corrosion, inhibitors, metal passivation, hydrophobization, carboxylic acids, carboxylates, amino acids.*

Received: September 1, 2016. Published: September 21, 2016.

doi: [10.17675/2305-6894-2016-5-4-1](https://doi.org/10.17675/2305-6894-2016-5-4-1)

Protection of metals by organic corrosion inhibitors (CIs) is based mostly on the adsorption of these compounds on a metal surface and subsequent formation of protective layers that minimizes access of corrosive ions to that surface. Adsorption can occur *via* electrostatic interaction of the CI with the metal substrate (physisorption), or it can involve charge sharing between the surface and CI (chemisorption), or combination of both interaction types can take place.

Passivation of metals remains a central problem to be solved by the corrosion science. In the development of nanoindustry methods focused on creating ultrathin layers on metals capable of preventing the corrosion of the metals, an important role is played by surface passivation using CIs. Corrosion inhibitors can form passivating (often polymolecular) layers on metals but with thickness $d < 10$ nm, making them invisible to an unaided eye and keeping intact the decorative properties of a coated article's surface. This passivation can be done using volatile CIs from the vapor phase or nonvolatile CIs from aqueous solutions. Since metal passivation using conventional corrosion inhibitors of oxidizing type (*e.g.*, nitrites, chromates) is seriously limited in practice due to environmental considerations, requirements for inhibiting formulations keep changing over time.

The use of corrosion inhibitors in passivation has played a major role not only in the application of oxidants (chromates, nitrites, *etc.*) but also in adsorptive, often “oxideless” passivation that we discovered as early as in the mid-1970s [1]. As for corrosion inhibitors

of adsorption type, the most important factor here is not metal oxidation, which can either be suppressed or not occur at all upon passivation, but the formation of a layer strongly attached to the metal surface, providing potential localization and blocking the percolation of corrosive medium components into it.

Over the past decades, the range of efficient organic passivating corrosion inhibitors was significantly expanded, allowing the environmentally hazardous oxidants to be replaced in many technological formulations and methods of metals protection.

In order to estimate the passivating properties of organic compounds towards metals in aqueous solutions, it is necessary, but not sufficient, to identify their ability to reduce the critical passivation current density (i_p). K. Schwabe [2] noted that oxidation of an iron surface changed the character of adsorption of organic inhibitors on it. In fact, dibenzylsulfoxide (DBSO) is firmly adsorbed by iron and is a good inhibitor. However, on oxidized iron, chemisorption of DBSO does not occur, therefore it is displaced by molecules of the solvent or corrosive components of the medium and becomes an ineffective CI. A different case is also possible. For example, it has long been known [3] that the benzoate anion does not slow down the active dissolution of iron in neutral aqueous solutions under naturally aerated conditions, or can even accelerate it, but it is able to prevent the disruption of the passive state of iron by corrosive anions such as Cl^- or SO_4^{2-} . Therefore, when a steel is covered by a natural oxide film, salts of benzoic acid (benzoates) often exhibit properties of corrosion inhibitors. Our adsorption study of organic CIs has also shown that they can be differently adsorbed from neutral aqueous solutions on a reduced (“clean”) and oxidized metal surface [1, 4–7]. In connection with this, it is important to find CIs that can be strongly adsorbed not only on a clean metal but also on an oxidized surface and stabilize its passive state due to a shift in the potential of local depassivation, E_{pit} , to more positive values.

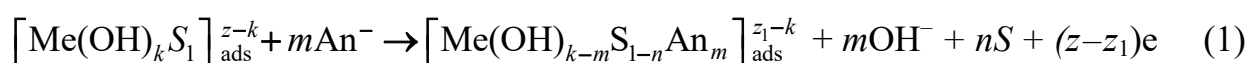
The chemical structure is an important factor in the choice of already known corrosion inhibitors or in the development of new CIs for various specific conditions. Determination of the quantitative dependence of the efficiency of CIs on molecular structure presents a fundamental challenge that researchers face, regardless of whether they study active metal dissolution, passivation, or localized corrosion.

A review of studies on the passivation of metals with organic CIs could make a whole monograph or several chapters in it. In this paper the author is limited to the most interesting classes of organic compounds that are already used in aqueous media or are promising for these media. In this report we will consider the effect of the chemical structure of one of the most thoroughly studied classes of organic compounds (carboxylic acids and their salts) on their ability to facilitate the passivation of various metals in aqueous solutions.

Monocarboxylates and amino acids. It is well known [1, 5, 8–10] that in the presence of some salts of weak carboxylic acids in neutral aqueous solutions the corrosion of iron and mild steels can be suppressed, *i.e.*, passivation takes place. Two mechanisms of the passivating action of carboxylates exist. The first one is associated predominantly with

the repair of defects and formation of insoluble deposits in the pores of the original air-formed oxide film and adsorption of inhibitor anion on the thin oxide layer [8, 10, 11]. As early as in 1975 [8], J.E.O. Mayne concluded that in aqueous solutions with pH 5–13, corrosion inhibition of iron was due to the fact that the air-formed oxide film was stabilized by the adsorption of a carboxylate or by local deposits of an insoluble ferric salt or a basic compound. The effect of a CI varies, depending on its chemical structure. Carbonates passivate iron at pH 11.1, borax at pH 9.2, but sodium azelate is capable of retaining passivating properties down to pH 5. The author explains the ability of anions to stabilize passivating oxide film by their control of the redox potential of the $\text{Fe}^{3+}/\text{Fe}^{2+}$ system. The easier the oxidation of Fe^{2+} to Fe^{3+} is, the faster insoluble compounds are formed. They plug the pores and defects of the passive film, *i.e.*, it is repaired. He noted also that sulphate, chloride and perchlorate are corrosive anions because of their inability to form a buffer, since they are salts of strong acids, and the formation of rust results in a steady fall in pH. This process leads to continuous corrosion.

We discussed the role of the chemical structure of anions in neutral aqueous solutions in iron passivation and inhibition of its local depassivation in detail in [1]. In considering metal depassivation we have introduced the concept of nucleophilic substitution of ligands (NSL) in a surface complex. In this concept, the anion is considered as the attacking nucleophile in the reaction:¹



From this it follows that the An^- displaces from the surface complex not only oxygen-containing particles such as OH^- but also molecules of solvent S (water or an organic compound). The behavior of a metal is thus determined by the reactivity of An^- and by the properties of the complex that is formed. If the latter is sufficiently stable and sparingly soluble, then the passive condition is stabilized, but the formation of a soluble complex will initiate the depassivation of the metal.

It was shown that the experimentally measured value of the local depassivation potential, E_{pit} , reflects not only the thermodynamics of complex formation, *i.e.*, its equilibrium potential $E_{\text{eq}} = E_{\text{Me}/\text{Me}^{n+}}^0 - RT/nF \ln(K_s a_{\text{An}^-} / a_{[\text{MeAn}]})$, but also the kinetic limitations for its occurrence. It follows that:

$$E_{\text{pit}} = E_{\text{Me}/\text{Me}^{n+}}^0 - RT/nF \ln(K_s a_{\text{An}^-} / a_{[\text{MeAn}]}) + \Delta + \eta_{\text{pit}}, \quad (2)$$

where Δ is the potential drop in the passive film – more precisely, in its defects – and η_{pit} is the overpotential, which depends on the nature of the metal and the activator. The nature of single-charged activator anions manifests itself in a difference in their affinity to water.

¹ Here the anion is shown as single-charged and the process as a single step, which is not always necessarily the case and is used here only for simplification.

It was shown that for the initiation of local depassivation on nickel by carboxylates of general formula RCOO^- in borate buffer with pH 7.4 and $C_{\text{An}^-} = 0.05 \text{ M}$, the E_{pit} value can be successfully described by the following equation:

$$E_{\text{pit}} = a - bf - c(2.6 + 0.6\sigma^* - 2.4E_s), \quad (3)$$

where a , b , c are constants for the reaction series; σ^* is the induction Taft constant of the substituent R; f and E_s are constants reflecting the hydrophobic and steric effects of R, respectively. From this, it is seen that the electronic σ -constants of R do not uniquely determine the reactivity of anions. It is necessary to consider the changes in the solvating effects. The concept of NSL in a surface complex shows the weak effect of the basicity of the An^- even more clearly if E_{pit} values are represented as a function of π and $\log MR$ only:

$$E_{\text{pit}} = a_1 - b_1\pi + c_1 \log MR, \quad (4)$$

where π is the hydrophobicity constant of an atom or a group of atoms constituting the anion [12] and MR is the molar refraction of the nucleophiles characterizing their polarizability. Although this equation is only applicable to single-charged anions, it does not require the knowledge of K_s , and the values of π and $\log MR$ of the corresponding atoms and groups are widely quoted [12]. Furthermore, in contrast to Eq. (3), it also covers anions of other chemical types: Hal^- , CNS^- , N_3^- , CN^- , NO_3^- , carboxylates, and sulfonates.

The validity of Eq. (4) has been checked in many metal oxide–solution systems, including the depassivation of not only metals (Fe, Ni, Co, Cu, Al, Sn) but also several alloys [1]. Moreover, it provides interesting information on the mechanism of the process. Thus, an increase in the hydrophobicity of the anion (the π -constants) is accompanied by a decrease in the value of E_{pit} , hence depassivation is facilitated; this effect is associated with a decrease in the energy barrier of the process. However, this effect is subject to limitations, since a further increase in the ligand hydrophobicity can lower the solubility of the complex and eventually lead to a change in the controlling stage, which changes to the transfer of the complex into the solution. Depassivation is then retarded when the hydrophobicity exceeds critical values of π_{cr} , so that Eq. (4) ceases to be valid at $\pi > \pi_{\text{cr}}$. The fact that an increase in the hydrophobicity of chemicals, for example monocarboxylates $\text{CH}_3(\text{CH}_2)_n\text{COONa}$, gives them passivating properties with respect to steels was evidenced by many authors in aqueous solutions under nearly neutral conditions [1, 10]. However, carboxylates with short chain lengths ($n < 4$) are less efficient and can be corrosive. Their homologues with $n > 4$ can form insoluble Fe(III) compounds and improve the repairing effect. If adsorption is weak even in this case, *e.g.* for hexanate, the solution pH should be increased in order to support the passivation of mild steel.

The value of π_{cr} characterizes the ligand hydrophobicity but also depends on the nature of the metal. In this situation, the range of corrosive ions differs significantly for different metals. Thus, for Cu and Ni it is significantly wider than for Zn and especially Sn, and this, at least in part, can be associated with an increase in the absolute values of the hydration energy, *i.e.*, the affinity for water of the cations of these metals, in the series:

$\text{Sn}^{2+} < \text{Zn}^{2+} < \text{Ni}^{2+} < \text{Cu}^{2+}$. Anions with $\pi > \pi_{\text{cr}}$ are usually classical CIs of localized corrosion and include higher alkylcarboxylates, amino acids and substituted benzoates.

The second case is less frequently encountered in practice than the first case. Here the passivation of a metal is provided by a firmly adsorbed organic corrosion inhibitor even when a “primary oxide film” is absent on the metal surface being protected. Its feasibility has been proved not only by laboratory tests [1, 3–5] but also by successful application of carboxylic passivators in industrial practice. For example, they are widely used in cooling lubricants, in which corrosion protection is subjected to the rapid renewal of the metal surface. Because of this and the possibility of high temperatures that may arise in the area of metal treatment, such as cutting or grinding, adsorption and other physicochemical phenomena may differ significantly from those on “usual” surfaces.

The role of the chemical structure of corrosion inhibitors belonging to different classes of carboxylates in their protective action on metals in neutral media was studied in detail in the last quarter of the 20th century. An important step in this research was made by using the well-known linear free-energy relationship (LFER) principle [13] to describe and predict the efficiency of corrosion inhibitors not only in the dissolution and passivation of metals or alloys, but also in the prevention of its local depassivation [1, 14, 15]. Over the past decade, the high passivating ability of various carboxylates and amino acids was proved not only for iron or low carbon steels [10, 16–22] but also for nonferrous metals [23–29].

At the same time, the opinion about the prevailing role of the basicity of carboxylic acids in determining whether their salts are CIs for mild steel can be found in the literature [30]. The passivation process depends significantly on the nature of the metal and the composition of its environment, especially the pH. For iron or mild steel, a minimum or critical pH value could be found in many cases, below which the passivation cannot occur. This value is given by

$$\text{pH}_c = \log c_s - \log c_{\text{O}_2} + \text{p}K_a + D \quad (5)$$

and depends on the nature of the weak carboxylic acid ($\text{p}K_a$), the concentration c_s of the salt, the content of dissolved oxygen c_{O_2} and the constant D which is related to the diffusion coefficients of oxygen and FeOH^+ species [10]. In an air-saturated solution at room temperature, Eq. (5) is reduced to:

$$\text{pH}_c = \log c_s + \text{p}K_a + 2.95 \quad (6)$$

Without denying the role of basicity, it should be noted that this simplification in the evaluation of the chemical structure of carboxylates offers little prospects. It is also necessary to take into account the second criterion, *viz.*, hydrophobicity of the molecules or the carboxylate anion, which is often more important than the $\text{p}K_a$ of the acid. The hydrophobic properties of a compound being studied can be estimated using the logarithm of its distribution coefficient $\log P$ in a system of two immiscible liquids, octanol–water [12]. This value allows one to calculate the characteristic magnitude of anion

hydrophobicity, $\log D$, taking into account the pK_a of the corresponding acid [31] and the solution pH:

$$\log D = \log P - \log[1 + 10^{\text{pH} - \text{p}K_a}] \quad (7)$$

For example, based on an analysis of adsorption and polarization studies, conclusions can be drawn regarding the important role of the hydrophobicity of anions in their effect on the passivation of low-carbon steel. As follows from the data presented in Table 1, sodium phenylanthranilate (SPhA), which has the lowest hydrophobicity of all of the monocarboxylates studied, passivates mild steel in a borate–chloride solution at the highest concentration C_{min} , *i.e.*, it is a relatively weak passivator under the conditions in question. Contrary to the authors [30], the sodium salt of rather a strong carboxylic acid (sodium fluphenamate, SFPh, *o*-[3-(CF₃)C₆H₄NH]C₆H₄COONa) is an efficient organic corrosion inhibitor, although the pK_a of the acid is below 4.0. It is easy to notice that the Cl[−] anion is characterized by an almost 2-fold higher value of $\log D$ than SPhA, *i.e.*, it is more hydrophobic. It is not surprising that other carboxylates that are more efficient passivators than SFPh, for example, sodium phenyl undecanate (SPhU), sodium oleate [C₁₇H₃₃COONa] (SOI) or sodium N-oleoylsarcosinate NaOOCCH₂N(CH₃)C(O)C₁₇H₃₃ (SOS), have even higher hydrophobicities.

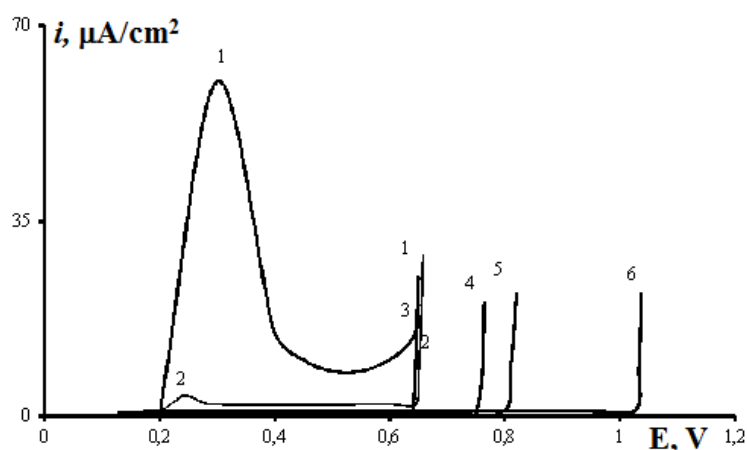
Among monocarboxylic acid salts, SOS is noteworthy. It is not only one of the most efficient water-soluble nonoxidative organic passivators for steels [18, 21, 35], but also has rather universal protective properties and prevents corrosion of Cu, Zn, Mg, Al and their alloys in corrosive neutral media [26, 36–38]. The high adsorption ability of SOS on steels has been known for a long time. This is not surprising, since SOS is known as a colloid surfactant that is used in a wide range of industrial applications because of its low toxicity [39]. Salensky *et al.* [35] studied the adsorption of SOS on mild steel from a heptane solution by means of ellipsometry, FT-IR and XPE spectroscopy. They argued that SOS chemisorption was due to the coordination of N and O atoms with the metal ions and formation of five-membered chelate rings. Later we have shown [21] that SOS is adsorbed substantially more strongly from a neutral aqueous solution on zone-melted iron in the absence of an oxide than on an oxidized surface of a similar electrode. The same phenomena are observed in the adsorption of SOS on a mild steel electrode (Table 1). However, even on oxidized steel, the free energy of SOS adsorption is high enough, ($-\Delta G_A^0$) = 38.9 kJ/mol, suggesting that chemisorption of the corrosion inhibitor occurs.

SOS also shows strong adsorption and a high passivating effect on Cu in borate buffer (pH 7.4) containing 10 mM NaCl. Among the sodium salts of carboxylic acids studied in [26], SOS demonstrated the best protective properties (Figure 1). Even at $C_{\text{SOS}} = 0.08$ mM, the passivation current density was reduced by a factor of 15 compared to the blank solution. When C_{SOS} increased to 0.17 mM, the CI was able to passivate Cu, although E_{pit} did not change, but at $C_{\text{SOS}} = 1.6$ mM, E_{pit} increased to 1.04 V.

Table 1. Protective effects of sodium carboxylates, values of their free energy of adsorption on low-carbon steel in borate buffer (pH 7.4) containing 10 mM NaCl, and their physicochemical characteristics.

Inhibitor of steel corrosion	Protective effects and $(-\Delta G_A^0)$ values in adsorption on low-carbon steel				Physicochemical characteristics	
	C_{in} for steel passivation, mmol/l	$(-\Delta G_A^0)$, kJ/mol at $E = -0.65$ V	$\Delta E = E_{pit}^{in} - E_{pit}^{bg}$, V at $C_{in} = 2$ mM	$(-\Delta G_A^0)$, kJ/mol at $E = 0.2$ V	pK _a of respective acid	log <i>D</i> at pH 7.4
SPhA	8.0	18.3	No	–	4.15 [32]	1.32
SMePh	6.0	27.4	0.14	29.3	4.33 [32]	2.29
SFPh	3.8	23.0	0.12	28.5	3.85[32]; 3.67	2.57
SPhU	1.0	31.3	0.15	30.2	4.78	3.30
SOI	1.10	40.2	0.16	34.0	5.02 [33]; 4.78	5.48
SOS	0.05	55.8	0.20	38.9	5.10 [34]; 3.55	4.03
Dimegin	0.08	78.3	0.20*	53.8	pK _a ¹ 4.30 pK _a ² 4.49	1.24

* This ΔE value was determined from the anodic polarization curves of low-carbon steel in the presence of 30 μ M dimegin.

**Figure 1.** Anodic polarization curves of copper in borate buffer solution with pH 7.4 (*I*) containing 10 mM NaCl and SOS (in mM): 0.08 (2), 0.17 (3), 0.40 (4), 0.80 (5), 1.60 (6).

Analysis of the results obtained by adsorption and polarization measurements demonstrates the important role of anion hydrophobicity in the ability to inhibit Cu dissolution. Interactions with the Cu surface are apparently due not only to the hydrophobic properties of a molecule but also to the presence of heteroatoms (particularly nitrogen) in its composition or multiple bonds that can form both additional intermolecular bonds between particles of an adsorbate such as SOS and other bonds with the metal

surface being protected. Results obtained by other investigators [40, 41] are in favor of this version. These investigations demonstrated the impact of the tail groups of SOS molecules on interactions with metal surfaces. For example, the role of amide bonds in the self-organization of surfactants on a gold surface was revealed in [40]. It was shown that sarcosine derivatives form chelate compounds with a metal surface that can induce the polymolecular adsorption of SOS molecules. Microbalancing was used to show that the ability to form hydrogen bonds resulted in more closely packed arrangements on hydrophobic surfaces. In [41] microbalancing and surface plasmon resonance were used to continue studies of the adsorption of surfactants – SOS and sodium salts of other amino acids, *e.g.*, *N*-lauryl sarcosine (NLS), from an aqueous solution on gold and quartz surfaces. All of these compounds contain polar tail groups with carboxylic groups that are attached to gold surfaces and form monolayers.

We have also shown using ellipsometric measurements [26] that SOS adsorption on Cu at $E = 0.0$ V is polymolecular in nature. The formation of the first monolayer of SOS started at an extremely low $C_{\text{sos}} = 0.05$ nM, and adsorption was described by the Frumkin equation with a relatively high value of $(-\Delta G_{\text{A}}^0) = 62$ kJ/mol indicating that chemisorption of SOS is possible. A multilayered film started to form after the formation of a monolayer ($C_{\text{sos}} \sim 0.12$ nM). It is important that SOS is adsorbed on Cu to a much greater extent than 1,2,3-benzotriazole (BTA), a well-known corrosion inhibitor of this metal, $(-\Delta G_{\text{A}}^0) = 51.3$ kJ/mol [41], and its alloys. Since BTA can generate multilayered films on Cu due to the polymerization of its complex with Cu cations [42, 43], the formation of multilayered coatings can be considered as a general and valuable feature of such different (in terms of chemical structure) inhibitors as SOS and BTA.

A confirmation of the high protective properties of SOS towards Cu was obtained by carrying out corrosion tests in an atmosphere with 100% relative moisture and daily water condensation on Cu samples [26]. The protective film was prepared by exposure for 5 or 60 min at room temperature or at elevated temperature (60°C) in a borate buffer solution containing carboxylates or BTA with $C_{\text{in}} = 2$ mM. Although the Cu plates were treated with very dilute aqueous solutions of the corrosion inhibitors, it was shown that SOS exceeded the other inhibitors studied in Cu protection from corrosion in a moist atmosphere. From the time to the occurrence of the first corrosion spot, it was concluded that, in the case where a protective film was formed at room temperature, the efficiency of SOS was 3 times higher than that of SPhA. The protection of Cu by SOS was likely to be accompanied by self-organization in adsorption layers, since the efficiency grew substantially along with the duration of the passivating treatment of Cu. It should be noted that the efficiency of treating Cu with SOS exceeded that of BTA. Raising the temperature to 60°C and passivation for 5 min increased the time until the first corrosion spots to 23 h instead of 10 h at room temperature in the case of SOS, and to 18 h instead of 12 h in the case of BT. Of course, there are several ways to improve the efficiency of Cu passivation by aqueous solutions of carboxylates, including SOS, which will be discussed below. Here, however, we note that among non-toxic carboxylates with sufficient hydrophobicity and an

adsorption-active functional group, corrosion inhibitors can be found that are at least no less efficient than the toxic chromates or heterocyclic inhibitors.

It has long been known that one of the efficient ways to prevent corrosion of Cu and its alloys is to provide hydrophobicity to their surfaces. Various wax compositions are widely used for this purpose, but in the last decade great attention has been paid to obtain stable superhydrophobic coatings that provide contact angles $\Theta_c \geq 150^\circ$ and a low drop rolling angle of such surfaces. Presently, it is believed that the superhydrophobic state is most efficiently achieved by rendering multimodal roughness to the surface and decreasing the surface energy of the processed material.

The multimodality of roughness should be characterized by the presence of texture elements on the surface, with sizes related to different spatial scales. Texture elements that have sizes from micrometers to hundreds of nanometers are usually combined in order to obtain such a relief, although other combinations of characteristic sizes are possible. For example, the well-known natural superhydrophobic surface of the lotus leaf is due to combination of texture elements with sizes of dozens of microns/microns/nanometers [44]. Authors [45] informed that they had developed a method of fabricating “stable superhydrophobic surface by merely immersing a copper plate (or substrate coated by copper) into a solution of fatty acid at ambient temperature.” The superhydrophobic properties result from a rough surface with cavities and mesopores or islands created in the etching process and the surface modification with a hydrophobic agent with low-surface energy provides a large Θ_c . After the surfaces are modified with it, the water droplet cannot get into the cavities or mesopores on the surfaces in which air is present.

In order to obtain $\Theta_c = 162 \pm 2^\circ$ on the surface of a Cu plate, it is placed in 0.01 M ethanol solution of tetradecanoic acid for 3–5 days at room temperature. During this time, the Cu surface takes on a specific morphology resembling a flower due to formation of $\text{Cu}(\text{CH}_3\text{C}_{12}\text{H}_{24}\text{COOH})_2$ clusters. Thereafter the samples are washed thoroughly with alcohol and deionized water, dried, and Θ_c is measured.

More detailed studies with processing Cu, Zn, and brass with ethanol solutions of various fatty acids (with C_6 , C_{10} , C_{14} and C_{18}) were conducted in [25]. The immersion times of metal specimens in ethanol solutions containing 0.01 or 0.10 M RCOOH were varied from 1 min to 6 days at ambient temperature. A positive effect of surface etching was shown in comparison with conventional sand paper cleaning. All carboxylic acids formed hydrophobic, self-assembled layers with $\Theta_c > 90^\circ$. However, superhydrophobization of Cu or bronze, *i.e.*, $\Theta_c \leq 115^\circ$, was not observed in any of the cases. The protective properties of the surfaces modified by fatty acids were determined on the basis of polarization curves of Cu in deionized water containing 0.2 g/L Na_2SO_4 , 0.2 g/L NaHCO_3 , and 0.2 g/L NaNO_3 . This solution (after adjusting the pH with 10% H_2SO_4 to pH 5) simulated the acid rain present in polluted urban environments. Carboxylic acids with longer carbon chains (myristic acid with C_{14} and stearic acid with C_{17} , SA) were better CIs. The formation of self-assembled layers was a rapid process, high inhibition efficiency values being observed even after 1 min of immersion. Myristic acid and, particularly, SA are good corrosion

inhibitors for Cu and brasses, providing protection above 95%, even at low molar concentrations. The time of immersion in ethanol solution affects the inhibition efficiency (Z , %) of carboxylic acids. Self-assembly can be a rapid process on Cu, an Z of over 87% being achieved after just 1 min immersion for Cu and brasses, and over 21% for Zn. A plate-like morphology, including nanoparticles, was formed on Cu in the case of SA, with the number of plates increasing with immersion time. This surface provided an efficient barrier to corrosive solutions. The layers formed on Zn show a much smaller number of plate-like products, indicating that the morphology affects the Z value.

For Zn, the difference between ground and etched samples is larger; etched samples showed a more positive corrosion potential and the Θ_c values on samples immersed in the SA solution were higher for etched samples (up to 122°). The Z of modified Zn samples increased with increasing carbon chain length from 23% for hexanoic acid to 49% for SA, but after 6 days of Zn immersion in ethanol solution of SA, when $\Theta_c = 128^\circ$, the Z increased to 58.4%.

It was recently shown [46] that the modified surface of Cu or Cu40Zn alloy became more uniformly covered upon addition of α -tocopherol (Vitamin E) in 0.05 M ethanolic solution of SA. It was made in order to obtain regularly ordered ridge-like or flower-like structures on the surface. Indeed, when 2.0% of α -tocopherol was added to the solution to modify the metal surface, the Θ_c on Cu increased from 138 to 143° . Upon treatment in a combination of SA and α -tocopherol, the corrosion potential of Cu increased with increasing $C_{\alpha-t}$. It became stable within a very short time after immersion of the sample in the solution that simulated acid rain.

Using polarization measurements and the EIS method in solution, the authors showed that the corrosion of Cu and Cu40Zn alloy decreased with increasing Θ_c . Since the prepared hydrophobic layers that contain α -tocopherol are more stable and have better inhibitive properties, this fact could be related to the esterification of SA and α -tocopherol. They explained it in terms of the higher adsorption ability of the “fatty ester” on the Cu and Cu40Zn surface with respect to the usage of SA or α -tocopherol alone as components that form the hydrophobic layer. The hydrophobic part also plays an important role in corrosion inhibition. Non-polar interactions between the long alkyl chains of the molecules due to van der Waals forces are also responsible for the protective quality because the hydrophobic part of the molecule prevents the access of water molecules to the surface. The Z value increased to more than 99%. This result seems to suggest that the film formed completely stops corrosion until degradation of the film begins.

G. Žerjav and I. Milošev [27] tried to increase the hydrophobicity of a Cu surface by modifying it not only with SA but also with a combination of SA with known heterocyclic CIs (BTA and 2-mercaptobenzimidazole, 2-MBI). In some experiments, samples were

² Z (%) = $[(i_{\text{cor}}^0 - i_{\text{mod}}) / i_{\text{cor}}^0] \cdot 100$, where i_{cor}^0 and i_{mod} are the corrosion current densities for a bare surface and for a surface modified by a CI.

placed for 1 hour into a 0.01 M ethanolic solution of BTA or 2-MBI followed by immersion them for 20 min into a 0.05 M ethanolic solution SA. In other experiments, samples were placed for 1 h in an ethanolic solution containing 0.01 M BTA or 2-MBI and 0.05 M SA. The morphology of the Cu layers formed upon modification in ethanolic solution of organic compounds is different, ranging from a flower-like structure for SA ($\Theta_c = 114^\circ$) to nanofibres for BTA ($\Theta_c = 90^\circ$) and nanograins for 2-MBI ($\Theta_c = 94^\circ$). When a Cu surface is treated with a combination of SA with BTA or 2-MBI, the layer hydrophobicity increases and Θ_c is $\geq 107^\circ$. The highest hydrophobicity was obtained by sequential immersion in a 2-MBI solution followed by immersion in 0.05 M SA ($\Theta_c = 118^\circ$). A 14-day corrosion test in the aqueous solution simulating urban rain (with pH 5) showed that a BTA layer acts as a strong activator of Cu corrosion. SA and 2-MBI layers inhibited corrosion. Binary and mixed combinations significantly reduced the weight loss of Cu samples and Z values between 72% and 93% were achieved for the 2-MBI+SA mixture. It is significant that it is only in the latter case that the surface of the samples even retained hydrophobic properties ($\Theta_c = 92^\circ$) after the test. The results of the electrochemical measurements on Cu electrodes with surface modified in solution simulating acid rain are in good agreement with the results of corrosion studies. The authors came to the conclusion that the layers formed by combinations of SA and CIs improved the protection of Cu and offered hydrophobicity as an additional functional property.

It should be noted that many carboxylates provide passivation and especially prevention of local depassivation of Fe and Cu relatively easily. However, efficient protection of Zn requires more hydrophobic carboxylates, *e.g.*, even SA is an insufficiently efficient passivator of Zn. As already mentioned above, amino acids may be more efficient CIs than fatty acids and their salts. In this connection, the authors [24] have studied the adsorption of SFPh from borate solutions on a Zn electrode at pH 7.4 and 9.1.

The previously obtained anodic polarization curves of Zn in a borate solution containing 10 mM NaCl showed that in neutral media the metal dissolved actively, but introduction of 1.6 mM SFPh was able to suppress the active dissolution. However, the stable passive state of Zn is disturbed by chlorides under anodic polarization. The potential of free Zn corrosion in weakly alkaline solution is significantly less negative, but in this case, even at low anodic polarization of the electrode, local depassivation of this metal is observed. The protective effect $\Delta E = E_{\text{pit}}^{\text{in}} - E_{\text{pit}}^{\text{bg}}$ increases with C_{SFPh} and is notably larger in the weakly-alkaline medium. In the neutral medium at $C_{\text{SFPh}} = 18.9$ mM: $\Delta E = 0.29$ V, while in alkaline medium even at $C_{\text{SFPh}} = 12.5$ mM: $\Delta E = 0.60$ V; no depassivation at $C_{\text{SFPh}} = 18.9$ mM is observed for Zn where $E_{\text{pit}} = 0.6$ V. Measurements of SFPh adsorption on oxidized Zn at $E = 0.2$ V justified the assumption about the better adsorptivity of the CI in weakly-alkaline solutions.

The film growth kinetics in borate buffer with pH 7.4 and 9.1 was studied using ellipsometry (Figure 2). In 120 min, in neutral solution, the film thickness attains 4 nm, while in alkaline solution it is close to 1.2 nm. The films formed in alkaline medium are

likely more compact, since they are thinner, and the CI is adsorbed intensely on such films. This is confirmed by the above mentioned fact of a greater increase at smaller C_{SFPh} values in comparison with neutral solution. In both cases, it is well described by the Frumkin equation:

$$BC = [\theta/(1-\theta)] \cdot \exp(-2a\theta), \quad (8)$$

where a is the attraction constant characterizing the interaction between the adsorbate particles and $B = 1/55.5 \cdot \exp(-\Delta G_A^0 / RT)$ is the adsorption equilibrium constant. The experimental data allowed us to calculate the adsorption constants: $(-\Delta G_A^0) = 57.8$ kJ/mol and $a = 1.7$ in the solution with pH 7.4, and $(-\Delta G_A^0) = 61.0$ kJ/mol and $a = 1.9$ in the solution with pH 9.1.

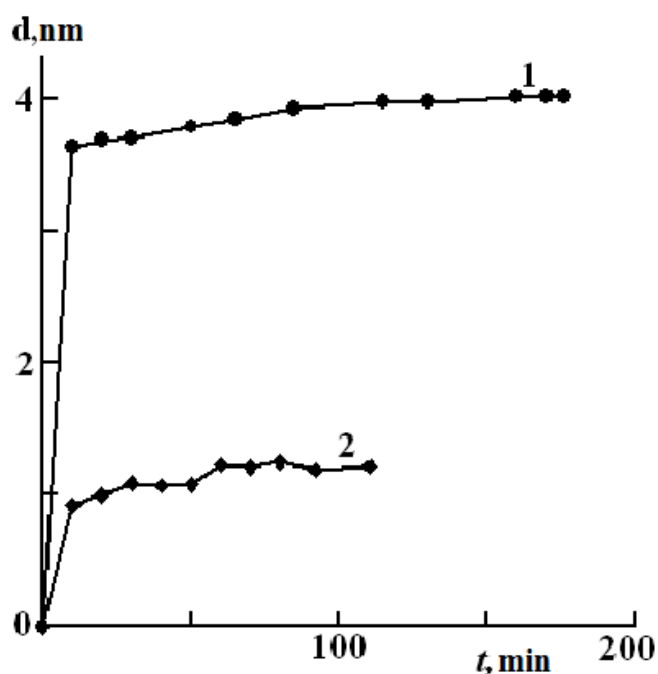


Figure 2. Kinetics of growth of oxide films on zinc surface in borate buffer with pH 7.4 (1) and pH 9.1 (2) at $E = 0.2$ V.

XPS surface studies gave additional information on the SFPh adsorption on Zn. Careful rinsing of the electrode with pure buffer solution and then with water in the XPS experiments showed that CI particles desorbed slowly. The nitrogen and especially fluorine heteroatoms in the SFPh molecule serve as label identifiers simplifying the interpretation of XPS results. The thickness of the SFPh layer depends as much as on the C_{in} in the solution as on the exposure time. The maximum thickness of the SFPh layer is somewhat smaller than the molecular length (1.4 nm), and close, within the experimental error, to the value obtained in the ellipsometric experiments. The SFPh anion is adsorbed through the carboxyl group $-\text{COO}^-$ and is perpendicular to the oxidized Zn surface. Figure 3 shows a side view of the possible arrangement of SFPh anions on the surface of Zn hydroxide.

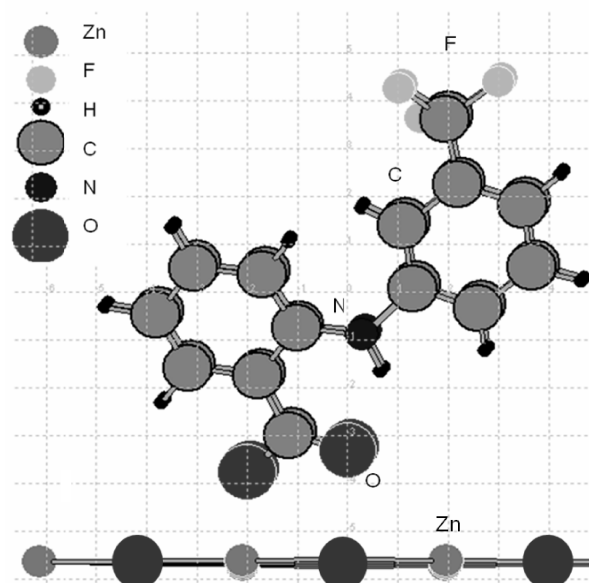


Figure 3. Possible locations of SFPh anions on Zn surface.

Recently [36] the protective and passivating effect of some sodium salts of higher carboxylates and sodium dioctyl phosphate on zinc in borate buffer solution with pH 7.4 was studied. We found that SOS has the best protection and adsorption properties (Figure 4). It was established that the adsorption of SOS on Zn is multilayered, that contributes to its best protection in anodic dissolution and in corrosion in a humid atmosphere with periodic moisture condensation on the samples. Treatment of Zn in aqueous solutions of the CIs increases the onset of the first corrosion damage on Zn in the humid atmosphere 2.5–4.5-fold. However, passivation of Zn even by efficient organic CIs such as SOS or SFPh cannot provide long-term protection of the metal in corrosive media.

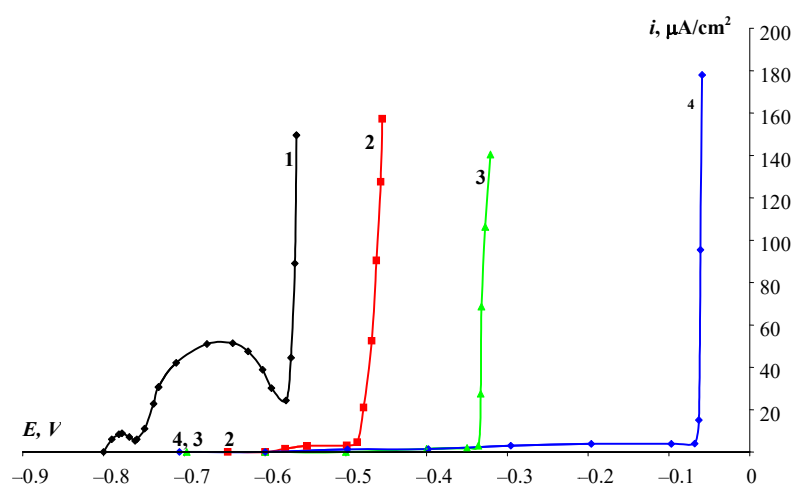


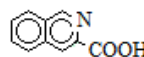
Figure 4. Anodic polarization curves of zinc in borate buffer solution with pH 7.4 (1) containing 10 mM NaCl and SOS (in mM): 1.0 (2), 5.0 (3), 10.0 (4).

In this regard, the work of K. Aramaki [47] is noteworthy where he carried out corrosion protection of Zn in a 0.5 M NaCl solution by treatment in a $\text{Ce}(\text{NO}_3)_3$ solution with subsequent modification in a solution of sodium hexadecanoate, $\text{C}_{15}\text{H}_{31}\text{COONa}$. Although the thin layer of hydrated Ce_2O_3 obtained on Zn as a result of the first stage of treatment was highly protective against Zn corrosion, no self-healing activity of the layer was observed [48]. To increase the protective properties of the hydrated Ce_2O_3 layer, the Zn electrode was modified by immersion in a methanol–water solution (2:1 v/v) of 0.1 mM $\text{C}_{15}\text{H}_{31}\text{COONa}$ at 30°C for various periods of time. The Θ_c value for Zn covered with a hydrated Ce_2O_3 layer was very low (about 9°), but when $\text{C}_{15}\text{H}_{31}\text{COONa}$ was adsorbed on the surface, the Θ_c value increased markedly to reach 113° in 71 h. The authors associated the increase in the hydrophobicity of the surface after its modification with a closer packing of carboxylate anions on Ce_2O_3 than on the Zn surface. X-Ray photoelectron and FTIR reflection spectra revealed that Ce_2O_3 layer contained small amounts of Zn^{2+} . The anions were adsorbed on the layer by formation of bidentate chelate bonds between Ce^{3+} or Zn^{2+} and COO^- . It was proposed that migration of $\text{C}_{15}\text{COO}^-$ adsorbed on the surface of Ce_2O_3 caused repassivation at layer defects, resulting in the maintenance of the passive state of the electrode and the high protection of Zn in 0.5 M NaCl against corrosion.

Higher carboxylates and amino acids have long been known as efficient CIs in neutral environments for Al, Mg and their alloys often referred to as “light alloys” [1, 49–53]. Among the numerous studies in the past decade concerning the replacement of CIs containing Cr(VI) by environmentally friendly salts of carboxylic acids, a further study of salts with a long carbon chain, *e.g.* sodium decanoate [54], may be noted. The authors have shown that the CI acts by forming a hydrophobic film on the surface of Al alloy AA2024 (shown by high values of $\Theta_c=115^\circ$ after immersion of a sample in a solution containing 0.1 M Na_2SO_4 + 0.05 M CI which strongly prevents attack of the passive layer by Cl^-). Electrochemical impedance measurements showed that the efficiency was high in a broad pH range (4–10). Special attention was paid to the action of the CI on intermetallic particles by performing local electrochemical impedance measurements in a model system (Al/Cu couple). It was shown that the CI was adsorbed on the surfaces of both metals, thus limiting the galvanic coupling responsible for the corrosion process.

Higher carboxylates can also be used for superhydrophobization of the surfaces of Al and its alloys, which should improve their corrosion resistance. For example, Al samples with purity 99.9% after anodization in 15 mass% H_2SO_4 were chemically modified in myristic acid with 10 wt% ethanol and 100 wt% molten myristic acid for 30 min at 70°C [55]. Subsequently, the samples were washed in ethanol at 70°C and deionized water and then dried in an oven at 80°C for 1 h. The Θ_c value for seawater on the surface was measured to be 154°. It was shown that a combination of anodization for 2 h with treatment of an Al sample by 100 wt% myristic acid is ideal for the formation of a stable superhydrophobic surface. Based on the results of analysis of potentiodynamic polarization curves, EIS and appropriate equivalent circuit models, the authors came to conclusion that

Al corrosion is efficiently inhibited by formation of a stable superhydrophobic film. Qi Wang *et al.* [56] reported the preparation of a superhydrophobic surface of Al alloy (mass%: 92.81 Al, 5.51 Cu and 1.68 Mg) after immersion of a sample in a solution of SA and *N,N'*-dicyclohexylcarbodiimide in *n*-hexane (5 mmol/l) for 24 h followed by drying in air. The value of Θ_c for the Al alloy sample was 156° . When samples of the Al alloy with superhydrophobic surface were immersed in water or aqueous solutions of salts (NaCl and Na_2CO_3) for 20 days, Θ_c decreased slightly (147°) in water. The authors came to the conclusion that the superhydrophobic surfaces of the Al alloy showed long-term stability and excellent resistance to corrosive liquids including acidic, basic and salt solutions.

Yet another approach was used in [57], where the authors also investigated the same AA2024 alloy but in an aqueous solution containing 0.05 M NaCl and organic complexing agents as corrosion inhibitors at $C_{in} \leq 0.05$ g/l. Comparison of EIS data showed three most efficient CIs: 8-hydroxyquinoline, salicylaldehyde, and quinaldic acid, . The CIs demonstrated superior suppression of corrosion in 14-day tests. It was concluded that the protective action of the CIs was based on the passivation of active intermetallic zones due to prevention of Mg, Al and Cu dissolution. Furthermore, the insoluble chelate layer prevents the adsorption of Cl^- on the alloy surface. The presence of the layer on the sample surface after its contact with a CI solution was proven by XPS analysis. Hence, quinaldic acid is a promising candidate to be added to coating systems for long-term anticorrosion protection of the Al alloy.

Certainly, the presence of an additional functional group close to the carboxyl creates additional possibility of sharing of the active center in the molecule of an organic CI. However, one should not exaggerate its role. In fact, Harvey *et al.* [58] have studied a range of structurally-related compounds for their capacity to inhibit corrosion of Al alloys AA2024-T3 and AA7075-T6 in 0.1 M NaCl solution. They found that the thiol group in the *para*- and *ortho*- positions to the carboxylate, and substitution of N for C in certain positions strongly inhibited corrosion. The hydroxyl group is slightly inhibitive, while the carboxylate group provided weak or no corrosion inhibition at all. However, there is not enough experimental data for a general conclusion to be made on the simultaneous involvement of two functional groups in the interaction of an organic CI with the metal surface being protected.

Possibly, a carboxylate that has the ability to form sparingly soluble compounds with Al^{3+} and cations of other metals the alloy contains, combined with high surface activity, *i.e.*, sufficient hydrophobicity of the CI itself, can be the most efficient CI for Al alloys. Although this condition is difficult to realize in practice, it indicates that efficient CIs may be found among anionic surfactants. In fact, sodium oleate (SOI) and its unsaturated homologues belonging to the class of carboxylates that have been investigated back in [1] provide an example of such efficient corrosion inhibitors for Al alloys. Recently, studies in this direction were continued in Ferrara University [59, 60] and in our laboratory [37].

A. Frignani *et al.* [59] evaluated the inhibiting action of some anionic surfactants (sodium salts of N-lauroylsarcosine (NLS), N-lauroyl-N-methyltaurine (NLT),

dodecylbenzenesulphonic acid (DBS), and sodium lauryl sulphate) towards AA2198 corrosion in 0.01 M NaCl solutions. They showed that these surfactants could slow down both the anodic and cathodic reactions of AA2198 alloy. It is important that these CIs noticeably shifted E_{pit} in the positive direction. Precipitation of their salts formed with Al^{3+} has the effect of pore plugging in the passive layer, and this increases the protective performance of the CIs. NLS and DBS that could withstand the effects of Cl^- were the most efficient compounds. It was noted that NLS acts through chemical adsorption on the Al alloy surface, while DBS and the other surfactants act through physical adsorption. Since their inhibiting action is related to the surfactant adsorption on the natural Al oxide layer, this different mode of interaction makes NLS a more efficient CI than DBS.

The same authors [60] continued to study the effect of NLS and DBS on the corrosion attack of an Ag-containing Al alloy (AA2139) during 168 h immersion in 0.01 M NaCl solution, and then compared these effects with those previously found on a Li-containing AA2138 alloy in the same environment. In this study, the different efficiency of the two additives was confirmed, highlighting their particularly strong effects on the alloy pitting process. The chemisorption of NLS is also more efficient for protection of AA2138 alloy than physical adsorption of DBS. In addition, since the passive layer of AA2198 is more protective than that of AA2139, the CI action is, in general, superior toward the former alloy than toward the latter one. The authors assumed that the CI effect on pitting depends on the density of cathodic Cu- and Fe-rich intermetallic precipitates: the higher this density (e.g., AA2139), the more difficult it is to suppress localized corrosion.

We have studied [37] another derivative of sarcosine (SOS), which, as shown above, has a high passivating activity on mild steel, Cu and a somewhat weaker activity on Zn. It was shown that the passivating film formed for 10 min at $t = 60^\circ\text{C}$ in an aqueous solution containing 16 mM SOS protects Al alloy AMg6 two times more efficiently than the film formed in a similar chromate solution. Testing the samples in a salt fog chamber also showed better protective properties of a SOS film in comparison with chromate passivation.

In the past decade, a significantly increased interest of researchers in finding efficient corrosion inhibitors for Mg and its alloys may be noted. Salts of higher carboxylic acids and amino acids were also studied. As early as in [53], it was found that among sodium salts of alkylcarboxylic acids with 7–12 carbon atoms, sodium undecanoate was the most efficient CI for a Mg alloy (15% Al, 3% Zn) in synthetic cooling water. Using Fourier Transform Infrared (FTIR) spectroscopy the formation of a layer of insoluble Mg undecanoate was revealed. Later [61] it was found that with an increase in the length of the hydrocarbon radical in higher fatty carboxylic acids with general formula $(\text{CH}_3(\text{CH}_2)_m\text{COOH})$, where $m = 10, 12, \text{ or } 16$, the anti-corrosion protection of Mg is improved. It was confirmed that the carboxylates were adsorbed from an ethanolic solution on the Mg surface and gave it hydrophobic properties.

F. Zucchi *et al.* [62] investigated the inhibiting effects of sodium salts of linear monocarboxylic acids toward AZ31 Mg alloy (2.5–3.5 Al, 0.7–1.3 Zn, 0.2–1.0 Mn, < 0.05

Si, < 0.01 Cu) in a saline solution (synthetic industrial cooling water). The length of the aliphatic chain in the acids ranged between 7 and 15 carbon atoms. The inhibiting action of these salts can be related to the precipitation of an insoluble Mg salt, which mainly affects the anodic reaction. The aliphatic chain length controls the anion solubility and the reaction rate of Mg carboxylate formation. This conclusion is in agreement with the results of Mesbah *et al.* [63], who also found that the inhibiting effect of carboxylates was due to a layer of insoluble Mg salts. Sodium octanoate is not a CI at all, while 0.01 M sodium decanoate rapidly forms Mg decanoate, but its protective effect substantially diminishes because the crystals do not form a very compact layer. The best inhibiting action is provided by 0.001 M sodium laurate. Its compact protective layer is formed in 12 h, afterwards the corrosion rates stabilize at a very low value ($Z > 90\%$). In the presence 0.10 mM sodium tetradecanoate, Mg myristate is formed more slowly and the protective effect increases steadily throughout the 96 hours of the test ($Z \sim 70\%$). However, the sodium salt of palmitic acid (C_{16}) does not have any protective action owing to its poor solubility.

Considering the above mechanism of corrosion inhibition of Mg and its alloys, higher alkylcarboxylic acids such as SA can provide good protection of these materials. It is very important for Mg application as an orthopedic implant, because SA is the main component of fat. That is why SA is nontoxic and biocompatible [64]. Magnesium is a potential candidate metallic material for degradable implants due to its valuable mechanical properties, non-toxicity, and degradability. However, the corrosion rate of Mg is too high. The SA coating can reduce the corrosion rate so that the implant can maintain sufficient mechanical integrity during the initial period of bone healing.

However, SA should not be applied to a surface to be protected from aqueous solutions, as in the protection of other metals. Since direct coating of Mg with SA is not possible due to poor adhesion, a two-step process was proposed in [65]. In the first step, Mg samples (99.96%) were subjected to a hydrothermal treatment at 120°C for 24 h to form an $Mg(OH)_2$ layer. In the second step, immersion coating was carried out under three different conditions of immersion: in 1.5 M SA solution in chloroform at 50°C for 2 h; immersion in liquid SA at 100 or 150°C for 2 h. The coating consists of SA anchored on $Mg(OH)_2$ grown by hydrothermal treatment, with formation of Mg stearate, which enhances the bonding. The thickness and quality of the SA coating depend mainly on the treatment temperature and on C_{SA} . The increase in corrosion resistance can reach as much as 4 orders of magnitude in the initial period and gradually drops to about 40 times in the long run. The authors found that degradation of the SA coating could be attributed to a local rise in pH and formation of corrosion products. They concluded that the SA coating enhances the corrosion resistance of an Mg implant so that it could provide mechanical support for bone healing.

Since reducing the weight of vehicles is important in order to decrease the fuel consumption and exhaust emission, the automakers are increasingly making use of light weight Mg alloys. ZE41 is a cast alloy, where Mg is alloyed with Zn, Zr and rare earth

elements. It is a widely used structural alloy in automobiles. The inhibitive action of sodium salts of SA, palmitic acid $C_{15}H_{31}COOH$ and miristic acid $C_{13}H_{27}COOH$ towards ZE41 alloy in an aqueous solution ($0.1\text{ M NaCl} + 0.2\text{ Na}_2\text{SO}_4$) at elevated temperatures of $30\text{--}50^\circ\text{C}$ was investigated [23]. It was shown that a proportional increase in Z was observed when C_{in} increased up to an $C_{in,max}$, beyond which the increase in Z was minimal. The $C_{in,max}$ is equivalent to the aggregate transition concentration of the carboxylate surfactants: it is 1.7 mM for stearate, 2.7 mM for palmitate, and 6.5 mM for miristate.

The adsorption of alkylcarboxylate anions is mainly physisorption and an increase in temperature leads to diminution of Z . They are chemically adsorbed only on intermetallic phases and inhibit the cathodic reaction by blocking the active reaction sites. Anodic inhibition is achieved through densification of the porous surface film by the precipitates of Mg carboxylates formed from physically adsorbed carboxylates. The difference in the Z and $C_{in,max}$ of the carboxylates is attributed to the difference in their aliphatic chain length which predominantly controls the solubility product of the corresponding Mg salts.

Helal and Badawy [66] investigated the corrosion inhibition of an Mg–Al–Zn alloy in stagnant naturally-aerated chloride-free neutral solutions using amino acids as environmentally safe corrosion inhibitors. The corrosion rate was calculated in the absence and presence of a CI using the polarization technique and EIS. The experimental impedance data were fitted to theoretical data according to a proposed electronic circuit model to explain the behavior of the alloy/electrolyte interface under various conditions. It was found that the corrosion rate depends on the adsorption of amino acid molecules on the alloy surface. Phenyl alanine has shown a remarkably high Z up to 93% at $C_{in} = 2\text{ mM}$. The corrosion inhibition efficiency was found to depend on the concentration of the amino acid and its structure. The mechanism of the corrosion inhibition process was discussed and a number of adsorption isotherms were investigated. The value of $(-\Delta G_{ad}^0)$ was calculated for the adsorption of various amino acids on the Mg–Al–Zn alloy and the values obtained reveal physical adsorption of the CI molecules on the alloy surface.

One of the best anionic corrosion inhibitors investigated for the protection of Mg alloy AZ31 in 0.1 M NaCl and $0.05\text{ M Na}_2\text{SO}_4$ solutions was the sodium salt of a sarcosine derivative, NLS [22]. Its protective effect was attributed to the rapid adsorption on the alloy surface, which limited the cathodic reaction, followed by a precipitation stage with Mg^{2+} that made the inhibiting layer thicker and less defective, so, in time, the anodic oxidation was almost blocked in a wide potential range.

Recently the influence of sodium salts of some higher carboxylates (sodium laurate, SL [$C_{11}H_{23}COONa$]; sodium linolenate, [$C_2H_5(CH=CH-CH_2)_3(CH_2)_6COONa$]; SOI and SOS) on the anodic dissolution of Mg-90 (Mg 99.9%; Fe $\leq 0.04\%$; Mn $\leq 0.03\%$; Al $\leq 0.02\%$; Ni $\leq 0.001\%$; Cu $\leq 0.004\%$; Si $\leq 0.009\%$) in borate buffer solution with pH 7.4 was studied in our laboratory [38]. Sodium oleate (SOI) was found to possess the best protective and passivating properties. The high protective properties of SOI were confirmed by exposure of Mg samples in a humid atmosphere with daily condensation of moisture on the samples. Preliminary passivation of Mg in an aqueous solution containing

16 mmol/l of SOI provides protection against the appearance of the first corrosion damage until 18–20 h, which is 6 times more efficient than passivation by chromates with the same concentration.

It is not to be supposed that only higher carboxylates or amino acids can be efficient CIs for the protection of Mg alloys. Recently a new concept was proposed for corrosion inhibition of the alloys [67, 68]. It takes into account the iron impurities in the Mg alloy that dissolve and form cations in the solution. These cations are reduced on the surface of the Mg alloy due to its very negative potential. This has the effect of enlarging the cathodically active sites on the surface and corrosion of Mg is drastically accelerated. In order to prevent iron re-deposition and decrease the area of cathodic sites, the authors introduced a strong Fe^{3+} complexing agent in the 0.5% NaCl solution. The pH of all 0.05 M solutions of iron complexing agents was adjusted by NaOH or HCl to a final value that varied between 7.5 to 5.9.

It turned out that all the iron complexing agents used efficiently lowered the corrosion rate of the Mg alloy. A correlation of inhibiting efficiency with the complex stability constants, $K_{\text{sFe}^{III}}$, was established. Sodium salicylate ($K_{\text{sFe}^{III}} = 36.8$) was one of the best CIs. The effect was slightly weaker in sodium oxalate solution ($K_{\text{sFe}^{III}} = 20.2$) and even lower in the case of sodium 5-methylsalicylate ($K_{\text{sFe}^{III}} = 9.77$).

Di- and polycarboxylates. This group of carboxylic corrosion inhibitors has been known for many decades [69–72], so in the past decade there was little research results that brought significant new information about the mechanism of corrosion inhibition or new possibilities for its use. However, it should be noted that the vast majority of studies were devoted to the passivating action of CIs with respect to Fe and various steels. Apparently, the absence of evidence of greater efficiency of the passivating action provided by di- or polycarboxylates as compared with mono-carboxylates is one of the reasons for the poor attention of researchers to these compounds.

Analysis of the role of the chemical structure of dicarboxylates in their protective effect is often limited to a comparison of the $\text{p}K_{\text{a}}$ values of the corresponding acids. As mentioned above, this factor is insufficient. Indeed, dicarboxylic acids $\text{HOOC}(\text{CH}_2)_n\text{COOH}$ are stronger than monocarboxylic acids. Sodium oxalate ($n = 0$, $\text{p}K_{\text{a}} = 1.23$) or malonate ($n = 1$, $\text{p}K_{\text{a}} = 2.8; 5.7$) are not corrosion inhibitors, but according to [8], sodium succinate ($n = 2$, $\text{p}K_{\text{a}} = 4.2; 5.6$), azelate ($n = 6$, $\text{p}K_{\text{a}} = 4.5; 5.5$) or sebacate ($n = 8$, $\text{p}K_{\text{a}} = 4.7; 5.4$) can be very efficient. However, the reason of changing the salt action mechanism may lie not so much in the growth of $\text{p}K_{\text{a}}$ values of the acid as in a decrease in the hydrophilicity of its anion, and hence, an increase in its surface activity. Furthermore, a decrease in the anion hydrophilicity can result in the formation of weakly soluble salts (or complexes) with cations of the dissolving metal.

With the proviso that the solution is naturally aerated, a high probability exists that insoluble Fe(III) carboxylate compounds would form, which are deposited at defect sites of the air-formed film. Thus, Rammelt *et al.* [19] used measurements of the dependence of the

free corrosion potential E_{cor} , anodic polarization of mild steel, and EIS to compare the corrosion protection of steel in aerated neutral solution (pH 7.5) by mono- (pelargonate $n = 7$, caprinate $n = 8$) and dicarboxylates (azelate $n = 6$, sebacate $n = 8$).³ Although all the investigated carboxylates are efficient in the presence of air, the authors found no advantages of dicarboxylates over monocarboxylates. They made the conclusion that the carboxylates act predominantly at local defects in the thin oxide layer by forming sparingly soluble Fe(III) compounds, in agreement with the pore plugging concept.

Valuable information was obtained by the EIS method in 0.01 M solutions of disodium sebacate and sodium caprinate. The authors [19] suggest that the impedance spectra obtained on mild steel in a neutral aqueous solution can be interpreted using a simple equivalent circuit with two time constants in parallel that represents an imperfectly covered electrode. The high frequency time constant ($R_{\text{ad}}/C_{\text{ad}}$) was attributed to the adsorption of an electrochemically indifferent substance. The low frequency time constant ($R_{\text{p}}/C_{\text{dl}}$) is related to the defect sites where charge transfer processes take place. In order to compare the different adsorption behavior in mono- and dicarboxylate containing solutions, the equivalent circuit was modified by a diffusion impedance. It could be caused either by the diffusion of soluble iron species from the electrode surface to the solution or by the diffusion of dissolved O_2 from the solution to the electrode surface (Figure 5). The diffusion impedance $Z_{\text{dif}} = W \cdot (j\omega)^{-0.5}$ (where the Warburg parameter is a measure of the diffusion resistance) was introduced in the equivalent circuit in parallel to the R–C circuit of adsorption. Both capacitances C in the time constants were replaced by a constant phase element CPE: $Z_{\text{CPE}} = A_{\text{CPE}}(j\omega)^{-\alpha}$. The CPE element is related to surface inhomogeneity resulting from surface roughness, adsorption processes or porous layer formation.

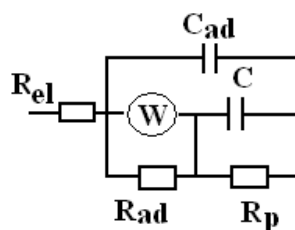


Figure 5. Equivalent circuit which represents an imperfectly covered electrode [19]. Here R_{el} is the solution resistance; R_{ad} and C_{ad} are the resistance and capacity that characterize adsorption; R_{p} and C are the charge transfer resistance and double layer capacity; and W is the Warburg impedance.

The capacitance values obtained in the low frequency range do not match those expected for C_{dl} and they ($21.2\text{--}24.4 \mu\text{F}\cdot\text{cm}^2$) almost did not depend on the carboxylate anion. In view of this, the authors assumed that these values are rather related to the capacitance of the iron oxide layer incorporating the insoluble Fe(III) carboxylates and interpreted the low frequency capacitance as C without the “dl” index. The R_{p} values in

³ Here n is the number of carbon atoms in the hydrocarbon chain of a mono- or dicarboxylate.

monocarboxylate solutions were significantly higher than those measured in the presence of dicarboxylates. This was explained by the different adsorption behavior observed in the high frequency range of the Bode plots. The adsorption resistance R_{ad} for dicarboxylates was lower than that for monocarboxylates indicating the poor adsorption ability of dicarboxylates. Even K. Aramaki and T. Shimura [73] who studied the behavior of α,ω -dicarboxylates assumed that they absorbed through both COO^- groups, which did not allow them to form a densely packed protective layer. German researchers [19] concluded on the basis of EIS analysis that the higher the value of R_{ad} , the more densely the adsorption layer is packed, and the lower C_{ad} , the more ordered the adsorption layer is. In the presence of azelate or sebacate, adsorption is weak and the adsorption layer does not act as a diffusion barrier. It is probably that is why the values of R_{ad} measured in the solutions of dicarboxylates studied were low and an additional diffusion impedance could not be found.

However, in our opinion, one should not neglect the higher dicarboxylates, which are still insufficiently investigated as CIs of passivating type. A protoporphyrin IX derivative [disodium salt of 2,4-di(1-methoxyethyl)deuteroporphyrin IX], dimegin (Figure 6), can serve as an example of a very efficient CI [17, 29,74].

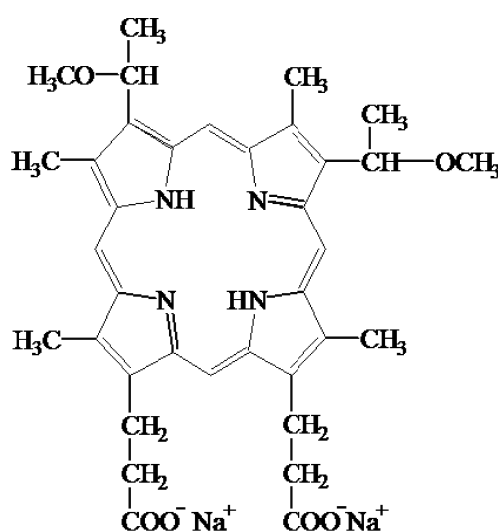


Figure 6. The structural formula of dimegin.

It follows from the analysis of the polarization curves shown in Figure 7a that at $C_{in} = 10 \mu\text{mol/l}$ of dimegin, the passivation current density i_p decreases from $83 \mu\text{A/cm}^2$, while E_{pit} increases by 0.070 V . At $C_{in} > 10 \mu\text{mol/l}$, the free corrosion potential increases, i_p becomes as low as $14 \mu\text{A/cm}^2$, and E_{pit} attains 0.25 V (at $C_{in} = 30 \mu\text{mol/l}$), while at $C_{in} = 80 \mu\text{mol/l}$, spontaneous passivation of steel is observed. It should be noted that C_{in} can be 3 orders of magnitude smaller than C_{NaCl} , but dimegin still increases E_{pit} . Apparently, at higher C_{in} , dimegin may stabilize the passive state of mild steel.

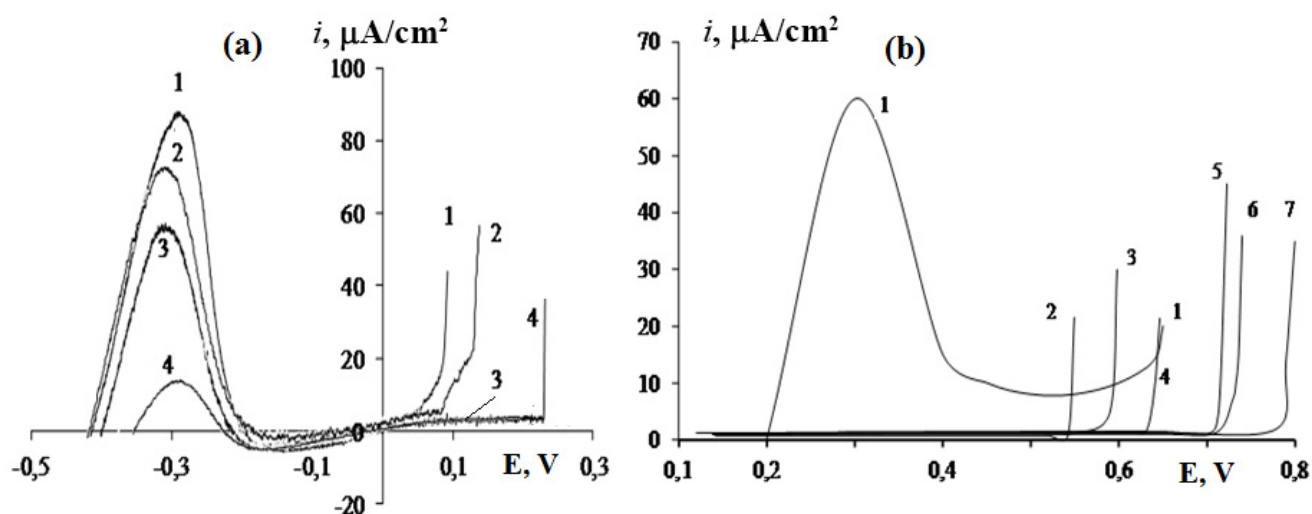


Figure 7. Anodic polarization curves of mild steel (a) and copper (b) in borate buffer (pH 7.4) containing 0.01 mol/l NaCl (1) and dimegin (in $\mu\text{mol/l}$) (a): 5.0 (2); 10.0 (3); 30.0 (4); and (b): 5.0 (2); 10.0 (3); 30.0 (4); 50 (5); 142 (6); 200 (7).

In studying the effect of dimegin on E_{cor} of Cu, it has been shown that its increase with time is stronger when the C_{in} is higher. Since dimegin is not an oxidizer, an increase in E_{cor} when it is added into solution indicates that it inhibits the anodic dissolution of Cu. Indeed, the anodic polarization curves in a borate buffer containing 10 mmol/l NaCl show that in contrast to mild steel, the Cu electrode is passivated in the presence of $C_{\text{in}} = 10 \mu\text{mol/l}$ ($\sim 6.6 \text{ mg/l}$) (Figure 7b). At C_{in} up to 30 $\mu\text{mol/l}$, the dimegin films formed passivate the surface, but, because of the branched structure of the dimegin molecule, the resulting layer is not thick enough to protect the surface from local depassivation by chlorides. Inhibiting the local depassivation of Cu requires that C_{in} be increased to 50 $\mu\text{mol/l}$, while the protective effect is $\Delta E = E_{\text{pit}}^{\text{in}} - E_{\text{pit}}^{\text{bg}} = 0.16 \text{ V}$.

The efficiency of dimegin in neutral solutions was compared with the known corrosion inhibitors for copper, *i.e.*, BTA, its derivative 5-chloro-1,2,3-benzotriazole (5-Cl-BTA), and the sodium salt of a monocarboxylic acid (SFPh), which is an efficient stabilizer of the passive state of metals [29]. In borate buffer (pH 7.4) containing 10 mmol/l NaCl, SFPh at $C_{\text{in}} = 140 \mu\text{mol/l}$ does not suppress the peak of the anodic dissolution of Cu, but E_{pit} reaches 0.43 V. It is somewhat lower than in the case of BTA: $E_{\text{pit}} = 0.46 \text{ V}$ or 5-Cl-BTA: $E_{\text{pit}} = 0.49 \text{ V}$. At the same C_{in} , dimegin provides significantly better stabilization of the passive state of Cu resulting in $E_{\text{pit}} = 0.73 \text{ V}$. Accordingly, the ability to stabilize the passive state of Cu increases in the order: SFPh < BTA < 5-Cl-BTA < dimegin.

Since the ability of dimegin to inhibit copper dissolution both in the active and in the passive states is related to its adsorption, we investigated the adsorption of dimegin on oxidized copper ($E = 0.0 \text{ V}$) in a pure borate buffer solution (pH 7.4) by *in situ* ellipsometric method. It turned out that dimegin adsorption occurred at low concentrations, $\log C_{\text{in}} = -7.75 \dots -5.75$, completing a conditional monolayer coverage of the electrode

surface. In this C_{in} range, the adsorption is adequately described by the Temkin equation with $(-\Delta G_A^0) = 56$ kJ/mol. Strong bonding of dimegin to the Cu surface suggests its chemisorptive character in the case of monolayer adsorption. Increasing C_{in} results in the formation of multilayers, probably due to the adsorption of copper complexes with dimegin formed in the solution.

Ellipsometric measurements allow calculating the thickness of a dimegin monolayer on the Cu surface at $E = 0.0$ V. It turned out that the monolayer thickness of dimegin should correspond to 0.65 ± 0.1 nm. This value is smaller than ~ 1.44 calculated from a model constructed and optimized with usual bond lengths. First of all, dimegin molecules may gather in clusters (islets) on the most active sites of the Cu_2O surface while leaving some parts uncovered. The molecules may be distributed evenly to form a loosely packed monolayer, and finally, the molecules may be inclined to the surface, giving rather a densely packed monolayer.

A study of the adsorption layer by an *ex situ* method, including a thorough washing of the electrode after removing it from the dimegin solution, was also performed. XPS is an independent method giving valuable information on the composition, oxidation state of atoms and thickness of thin surface layers. Since the method requires removal of an electrode from a solution, it is very important to choose the exposure time of a sample in a solution. For this purpose, data on the kinetics of the change in the ellipsometric angle Δ in the CI solution with $C_{in} = 10$ $\mu\text{mol/l}$ was used. As seen from the Δ^0 change, a formal monolayer of dimegin on Cu was formed in 40–60 min at this concentration (Figure 8). Taking this finding into account, the sample was exposed in solution for 60 min for XPS measurements.

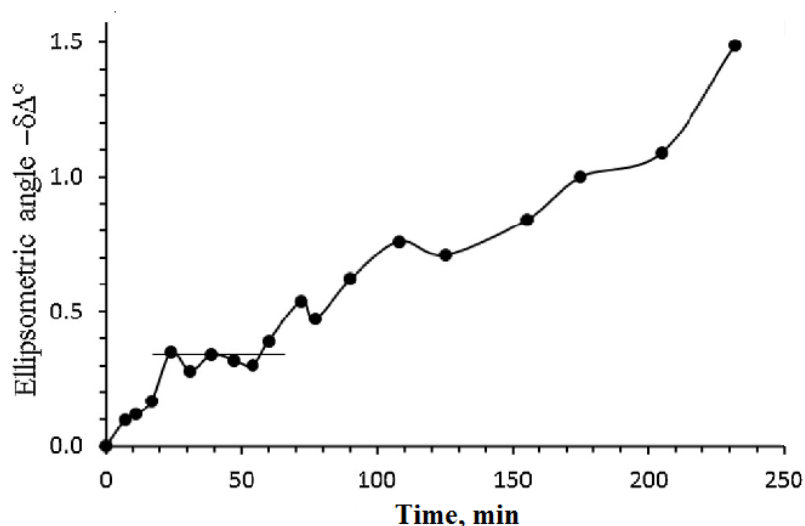


Figure 8. Change of kinetics of ellipsometric angle Δ^0 for oxidized Cu ($E = 0.0$ V) upon dimegin addition ($C_{in} = 10$ $\mu\text{mol/l}$). The angle corresponding to a formal monolayer coverage by dimegin on the oxidized surface of Cu is shown by a horizontal line.

XPS studies suggest that dimegin is bonded to surface copper cations through two oxygen atoms of the carboxyl groups. The nitrogen atoms are not involved in the formation of coordination bonds with copper cations. Based on the integral peak intensities of all elements making up the surface, the thicknesses of the dimegin layer (1.0 ± 0.3 nm) and a Cu_2O layer (1.7 ± 0.3 nm) were calculated using the MultiQuant program. The estimated thickness of the dimegin monolayer is comparable with its ellipsometric measurements made *in situ*. It also confirms the validity of our assumptions about the chemisorption of dimegin because thoroughly washing the Cu surface and placing the electrode in a vacuum has virtually no effect on the assessment of the amount of adsorbed dimegin. The adsorbed dimegin anions are probably at a slanted orientation relative to the Cu surface.

The adsorption behavior of dimegin on mild steel studied in detail with the use of ellipsometry in borate buffer (pH 7.4) also leaves no doubt in its chemisorption. It should be noted that adsorption of dimegin on zone-melted iron and mild steel is described by the Temkin isotherm (Table 2) [74]. From consideration of the research results presented in Figure 9 it follows that in both cases dimegin is better adsorbed on the electrode surface at $E = -0.65$ V than on a pre-oxidized surface, *i.e.*, at 0.2 V. Upon adsorption, dimegin forms strong bonds with the steel surface, particularly noticeable for oxidized steel. Furthermore, at this potential adsorption on iron is not limited by monolayer formation, since on further increase in C_{in} , the $\delta\Delta$ value starts to grow again. It is possible that this is due to the formation of associates of dimegin [75] or its adsorption complexes with iron cations, just as it was observed in adsorption of triazoles on copper [76]. Perhaps, the more dense packing of the monolayer adsorbed on steel prevents the transition of metal cations into the solution and the formation of their complexes with dimegin, which then would be able to be adsorbed on the electrode surface. It is no coincidence that the Δ changes on steel surface reach *ca.* -1.40° , which corresponds to the film thickness of 1.5 nm and suggests a vertical orientation of dimegin particles in the monolayer. On iron, $\delta\Delta \sim -0.95^\circ$ under the same conditions, which corresponds to a layer thickness of 1 nm, *i.e.*, dimegin particles are adsorbed obliquely.

Table 2. The values of the adsorption characteristics for dimegin on metals with different potentials.

Metal, potential of electrode in borate buffer	f	$(-\Delta G_A^0)$, kJ/mol
Zone-melted iron ($C < 0.0013\%$), $E = -0.65$ V	1.6 ± 0.4	73.8 ± 3.7
Mild steel St 3, $E = -0.65$ V	3.3 ± 0.2	78.3 ± 3.9
Zone-melted iron, $E = 0.2$ V	1.0 ± 0.1	43.3 ± 2.2
Mild steel St 3, $E = 0.2$ V	2.2 ± 0.3	53.8 ± 2.7
Mild steel St 3; borate buffer + 0.9 or 2.5 mmol/l NaCl, $E = 0.2$ V	3.5 ± 0.3	53.0 ± 2.6
Mild steel St 3; $E_{\text{cor}} = 0.18$ V (without polarization of the electrode)	2.3 ± 0.2	50.6 ± 2.5

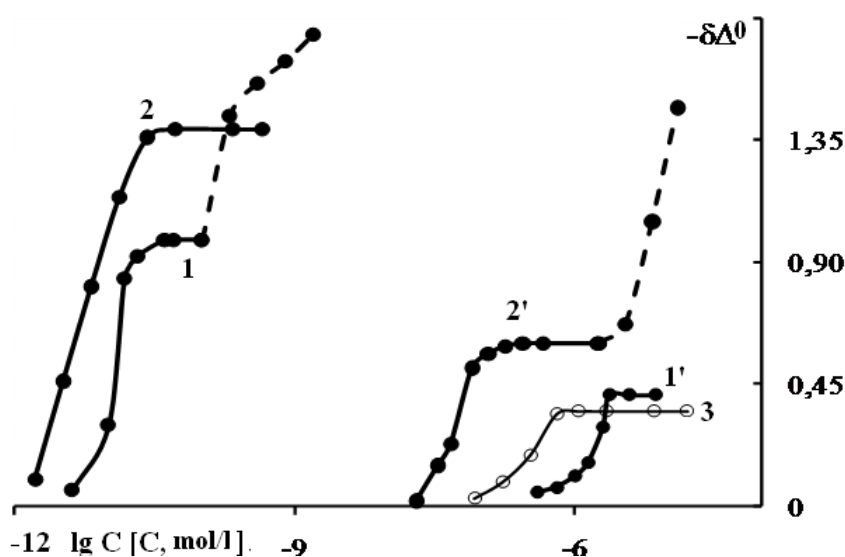


Figure 9. Dependence of change in ellipsometric angle $\delta\Delta^\circ$ upon dimegin adsorption on zone-melted iron (I, I') and mild steel St3 ($2, 2', 3$) in borate buffer with pH 7.4 on dimegin concentration. Curves I and 2 were obtained at $E = -0.65$ V and curves $I', 2'$, at $E = 0.2$ V. Curve 3 was obtained at $E_{\text{cor}} = 0.18$ V (after exposure of the electrode in the solution for 1 day).

At $E = 0.2$ V, the conditional monolayer thickness on the surface of iron is ~ 0.4 nm, and the thickness of the monolayer on steel surface is higher (0.6 nm) than on iron, but smaller than at $E = -0.65$ V. Hence, the orientation of adsorbed dimegin anions on iron can be almost parallel to the surface.

Further exposure of an oxidized iron electrode in a solution with the addition of the CI ($\log C = -4.33$) for 29 hours shows no signs of the formation of a second layer that could consist of soluble complex compounds of dimegin. It is possible that if dimegin complex compounds are formed, this occurs directly on the electrode surface rather than in solution. It is significant that, unlike the active dissolution of iron that occurs through formation of Fe(II), *i.e.*, complexing cations, the dissolution of the metal from the passive state occurs only through the transition of Fe(III) into the solution. On the contrary, for St3 at $E = 0.2$ V, an increase in $\delta\Delta$ is observed after a monolayer has been filled ($C_{\text{in}} > 1$ mmol/l). This can be explained by a more inclined orientation of dimegin anions on the electrode surface and formation of a less dense first layer. Nor can it be ruled out that in the case of steel, complexation with cations of other metal contained in the steel takes place.

As it turned out, the saturation of the adsorption layer on mild steel at E_{cor} is approximately in the same C_{in} region as in case of dimegin adsorption on steel surface pre-oxidized at $E = 0.2$ V. The values of $(-\Delta G_A^0)$ for E_{cor} and $E = 0.2$ V are similar: 50.6 and 53.8 kJ/mol, respectively (Table 2). These measurements are noteworthy because they show that the oxide film naturally growing in borate buffer adsorbs dimegin like an electrode that underwent a preliminary complex and lengthy treatment at $E = 0.2$ V. In all

cases, the results clearly show that dimegin is strongly adsorbed not only on an active electrode but also on a passive one, *i.e.*, in a wide range of potentials ($E = -0.65$ to 0.2 V).

The values of $(-\Delta G_A^0)$ suggest that chemisorption of dimegin occurs on the electrodes that we have studied. To test this assumption, it was of interest to study the protective “aftereffects” of dimegin adsorption on an oxidized steel surface exposed to a corrosive sodium chloride solution. For this purpose, St3 electrode was submerged into a borate buffer solution (pH 7.4) at $E = 0.2$ V containing dimegin so that its C_{in} (1 mmol/l) provided the formation of a monolayer of the CI on the steel surface. After establishing a constant Δ (in 2 h), without disconnecting the potential provided by the potentiostat, the cell volume was washed three times with borate buffer. The electrode was left for a day in this solution to determine the reliability and constancy of Δ and the absence of dimegin desorption from the electrode surface. After that, a concentrated NaCl solution was introduced into the solution to reach $C_{Cl^-} = 2.5; 5.0; 7.5; \text{ and } 10.0$ mmol/l in the cell, and the Δ value was measured as a function of time.

For a period of 10 h, chloride at concentrations $C_{Cl^-} \leq 2.5$ mmol/l does not cause the breakdown of both the oxide film and the passive electrode surface modified by 1 mol/l dimegin. If a St3 electrode is not subjected to pre-adsorption of dimegin, then in 65 min after addition of chloride to the solution ($C_{Cl^-} = 5.0$ mmol/l), local depassivation of steel is observed. An electrode coated with a conventional monolayer of dimegin, despite a 3-fold longer exposure followed by washing in pure buffer, showed no sign of depassivation even 6 h after the addition of NaCl. Upon increasing C_{Cl^-} to 10 mmol/l, local destruction of the protective layer formed by dimegin occurs in 10 min. Without adsorbed dimegin, breakdown of the protective layer started immediately, *i.e.*, less than in 1 min, after NaCl addition to the solution. The results of these experiments support the hypothesis on the chemisorption nature of the interaction of dimegin with steel surface.

It can be assumed that at $C_{Cl^-} \leq 2.5$ mmol/l, chloride is adsorbed on the steel surface, although in insufficient quantity to cause the formation of corrosion in a defect of the oxide film. Indeed, it is seen that upon dimegin adsorption on steel pre-exposed in a borate buffer solution (pH 7.4) containing 2.5 mmol/l NaCl, the magnitude of $|\delta\Delta|$ at the same C_{in} is lower than that upon adsorption on oxidized steel without prior chloride addition.

It is characteristic that the shape of the isotherms remains the same. The adsorption isotherms of dimegin on steel in all the cases studied (with and without partial coverage of its surface with chloride) lie in the same area of C_{in} . In this connection, it was suggested that at this C_{Cl^-} adsorption of Cl^- only changes the spatial orientation of the dimegin particles in the adsorption layer on the steel surface.

The results of adsorption and electrochemical studies of dimegin allow us to come to an important conclusion. The introduction of two carboxyethyl groups in the hydrophobic macrocycle allows us to create a sufficiently soluble reagent in water, that is capable of very efficient passivation of various metals due to firm chemisorption and high shielding

effect of large molecules. It is noteworthy that despite the relatively high hydrophobicity of the dimegin molecule (an approximate calculation gives $\log P = 6.4 \pm 1.4$), its anion has the lowest hydrophobicity among the carboxylates studied by us (Table 1). This explains the fact that dimegin is dissolved in a neutral aqueous solution sufficiently to be one of the most efficient passivators for mild steel, and free energy of its adsorption is even higher than the same value of the other carboxylates discussed in our paper.

The high adsorption ability of dimegin on various metals and in a wide range of electrode potentials may be useful not only for their passivation in aqueous solutions but also for surface modification with subsequent adsorption of other commercially available corrosion inhibitors. Indeed, we have shown that preliminary adsorption of dimegin on Fe [17] or Cu [29] can improve BTA adsorption. For example, if a Cu or Fe surface is pre-modified by dimegin chemisorption, BTA adsorption on the surface is improved. The adsorption of BTA on passive Fe, Cu and their surface preliminarily modified by chemisorption of dimegin can also be adequately described by the Temkin equation.

Dimegin stimulates the adsorption of BTA, as indicated by a shift of the adsorption isotherms for BTA on the surface with pre-adsorbed dimegin, even when $\Theta_{\text{DMG}} = 0.1$, towards the concentrations where BTA adsorption on a passive Cu surface does not occur. Preliminary chemisorption of dimegin obviously enhances the subsequent BTA adsorption, which is characterized by a higher value $(-\Delta G_a^0) = 63$ instead of 58 kJ/mol. The factor of surface energetic heterogeneity, *i.e.*, value f in Temkin equation, also increases: 2.4 and 5.4, respectively. Corrosion tests confirmed an improvement in the protective properties BTA after previous adsorption of dimegin on Cu. A copper plate treated with a dilute BTA solution (1 mmol/l) and then placed in a chamber with periodic condensation remains completely protected for several days: the first corrosion damage was noticed after 9 days. If it is pre-kept in a dimegin solution with a concentration (at least $\log C = -8.1$), which corresponds to $\Theta_{\text{DMG}} = 0.47$, and then treated with a solution of BTA (1 mM/dm³), the period before the appearance of the first corrosion damage in the humid chamber becomes two times longer.

An even more pronounced surface modification by dimegin is observed in the case of Fe. The modification of the surface of passive Fe by dimegin adsorption was carried out at $E = 0.2$ V; then the solution was replaced with the pure borate buffer without switching off the potentiostat. To measure BTA adsorption on the surface of the modified electrode, we added concentrated BTA in portions to pure borate buffer, then measured the changes in the ellipsometric angle Δ in time. When Δ reached a constant value, we regarded it as a criterion of equilibrium BTA adsorption.

The dependence of $\delta\Delta$ on the logarithm of BTA concentration can be regarded as the isotherm of its adsorption on the surface of iron modified by dimegin (Figure 10). All the isotherms obtained in this way are adequately described by the Temkin equation. The adsorption parameters calculated according to it are listed in Table 3. Small changes, $|\delta\Delta| \sim 0.18^\circ$, upon the adsorption of BTA on oxidized Fe correspond to a film thickness of 0.4–0.5 nm, which attests to the planar location of a BTA molecule on the surface of oxidized

iron. However, the thickness of the adsorbed BTA layer significantly increases when it is formed on oxidized Fe (at the same $E = 0.2$ V) whose surface was at least partially pre-filled by adsorbed dimegin. At all degrees of coverage with dimegin Θ_{DMG} that we studied, the thickness of the adsorbed BTA layer lies within the region of 1–1.2 nm.

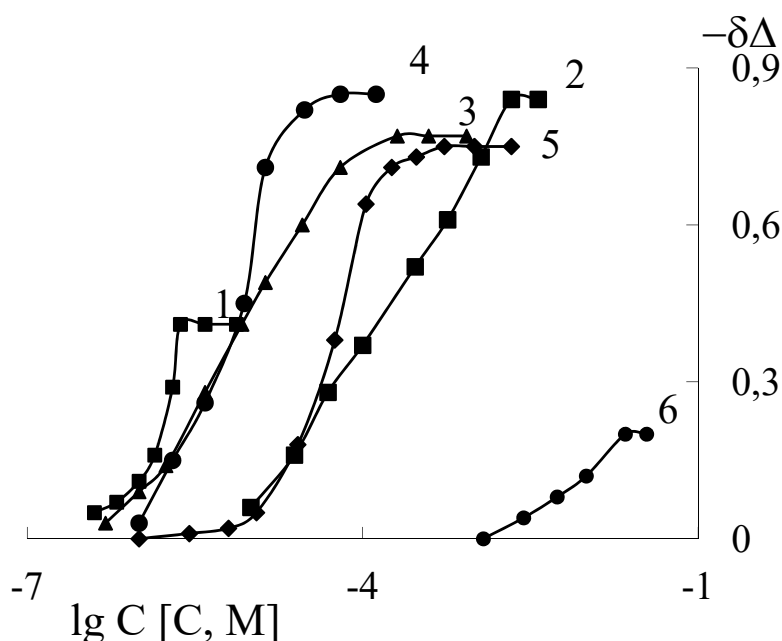


Figure 10. Change in ellipsometric angle $\delta\Delta$ as a function of logarithm of C_{DMG} (1); C_{BTA} (6) on Fe surface oxidized at $E = 0.2$ V; and C_{BTA} on an iron electrode preliminarily modified by dimegin adsorption. Degrees of coverage of the surface with the electrode, θ_{DMG} : 0.27 (2); 0.50 (3); 0.70 (4); and 1.00 (5).

Table 3. Adsorption characteristics of BTA upon variation in degree of coverage of oxidized iron surface with dimegin.

Θ_{DMG}	f	$(-\Delta G_{\text{a}}^0)$, kJ/mol
0.00	3.6 ± 0.7	19.2 ± 0.9
0.27	5.1 ± 0.3	38.7 ± 1.9
0.50	5.0 ± 0.5	45.1 ± 2.2
0.70	1.9 ± 0.5	44.6 ± 2.2
1.00	4.7 ± 0.8	39.9 ± 2.0

The observed increase in $(-\Delta G_{\text{a}}^0)$ value and strengthening of BTA binding with the iron surface can arise not only from the possibility of the formation of its associates with chemisorbed dimegin anions, but also from the general change in the energy state of the

electrode surface itself. In this respect, the change in adsorption parameters of BTA as a function of Θ_{DMG} is demonstrative.

The increase in the f value in the adsorption isotherm of BTA upon transition to the modified surface can be easily understood, since adsorbed dimegin occupies only a small fraction ($\Theta_{\text{DMG}} = 0.27$) of the total surface (Table 3). At $\Theta_{\text{DMG}} = 0.50$, the $(-\Delta G_a^0)$ value is maximal. Here, the tendency for f to decrease begins to emerge, although to a negligible extent. The further increase in θ_{DMG} attests to this tendency and results in a decrease in $(-\Delta G_a^0)$, which indicates an attenuation of BTA adsorption. In the first approximation, one may assume that a surface not filled with dimegin is also capable of somehow facilitating BTA adsorption. Although the explanation for this phenomenon requires further studies, it may be assumed that the lateral interaction of the aromatic systems of both CIs, strengthening the BTA adsorption on Cu or Fe electrode coated with “islets” of adsorbed dimegin, is an important factor.

Thus, the possibility of high passivating properties of dicarboxylates, as shown by the example of dimegin, is still far from being exhausted. It should be noted that the protective properties of dicarboxylates with respect to non-ferrous metals and alloys and the role of the chemical structure of a CI have practically not been studied. In addition, we have considered the above dicarboxylates in which adsorption and passivation of metals was associated only with their anions, but it has long been known that some metal cations such as Ca^{2+} , Zn^{2+} or Ce^{3+} are able to enhance the protection against corrosion in neutral solutions [1, 77].

Although metal cations themselves cannot passivate mild steels in neutral solutions, since the principle of their protective action is mainly to slow down the cathodic reaction due to deposition of sparingly soluble hydroxides on the surface to be protected, their formulations with anionic organic corrosion inhibitors are often better protectors, *e.g.*, of mild steels. An example of such a formulation is a mixture of the sodium salt of adipic acid (SAA) with ZnSO_4 that was studied as a CI to protect mild steel in hard water containing 0.665 ppm Cl^- and 14 ppm SO_4^{2-} [78]. It was found that the formulation of 200 ppm SAA with 50 ppm ZnSO_4 provides almost complete protection of steel ($Z = 98\%$) due to the synergistic action of its components. It is a mixed CI since it inhibits both electrode reactions on steel. FTIR spectra reveal that the protective film formed by the CI on the steel consists of $\text{Fe}^{2+} - \text{AA}$ and $\text{Zn}(\text{OH})_2$, *i.e.*, protection of steel proceeds according to the well known mechanism of action of many Zn-containing compositions or complexonates, as discussed in detail in [1].

It should be noted that a similar mechanism of protection can be realized in the case of polycarboxylates, among which polyacrylic, polyaspartic and 2-phosphonobutane-1,2,4-tricarboxylic acids as well as their zinc complexes are most famous [1, 79, 80].

Mixtures of carboxylate CIs. It is well known that some of them are capable of facilitating the passivation of metals better than the components of the blend [1, 77, 81–85]. It has been known that to improve the passivating effect of a carboxylate with respect

to iron or mild steel, its combination with an oxidizer can be used. For example, we have shown that a stronger oxidizer, sodium nitrophthalate, in very small quantities (>0.2 mM) has a beneficial effect on the passivation of iron in neutral phthalate solutions [85]. Phthalate ions are strong stimulators of the active dissolution of iron, evidently as a result of the ease of transfer of the surface compounds that they form into solution. This dissolution prevents the organic anion from fulfilling its passivating function. On the other hand, its adsorption is accompanied by a fall in the surface concentration of the passivating components of the solvent which leads to an increase in the critical current density for passivation, i_p . With sodium nitrophthalate present in the solution, the deficiency of passivating components can be made up by the accumulation of OH^- resulting from the accompanying cathodic reaction. In this case, the negative effect of the lower arylcarboxylate on the passivation of iron is reduced or disappears completely. For oxidizers, where the rates of reaction increase with temperature and cause the generation of OH^- , one can expect a beneficial effect on the efficiency of CIs of the adsorption type. The combined effect of nitrophthalate with SPhA on the initiation of pitting on iron can serve as the simplest example [1].

Yet another way to improve the passivating action of CIs of the carboxylate type is by combining them with another carboxylate that is not an oxidizer. Thus, passivation of mild steel or aluminium alloys by binary CIs such as SPhA with SOL, even at a low total concentration, can be more efficient than that given by the better of the individual CIs, *i.e.*, SOL [1, 7, 86]. A feature of this system is that even better results are obtained by replacement of SPhA in the mixed CI by a more efficient passivator, *e.g.* SFPh [86]. Among the CIs studied, the mixture of SFPh with SOL is the most efficient one for iron passivation and its protection from local depassivation, which can be explained by the better adsorbability of the organic anions.

Among other salts or higher carboxylic acids mixed in certain proportions in order to improve passivation of mild steel, one can mention the mixture of SMePh with sodium hydroxynaphthoate $\text{C}_{12}\text{H}_6(\text{OH})\text{COONa}$ (SONP) [87]. The carboxylates cannot compete with each other in adsorption, but their equimolar mixture protects steel better than the components do separately. They possess almost equal $(-\Delta G_a^0) \sim 27$ kJ/mol, but their mixture is better adsorbed on the surface. To suppress the corrosion of a rotating cylinder made of mild steel in neutral solution, the corresponding value of C_{in} for the mixture is half that for each carboxylate (Figure 11).

Recently it was found [19] that the adsorption ability of dicarboxylates is weak, but the corrosion protective effect could be improved considerably if mixtures of dicarboxylates with monocarboxylates are used. The additional inhibition effect was ascribed to the ability of monocarboxylates to adsorb stronger on the oxide-covered mild steel surface than dicarboxylates. The sebacate/caprylate mixture provides the best protection comparable with the synergistic effect observed with carboxylate in the presence of benzotriazole, too.

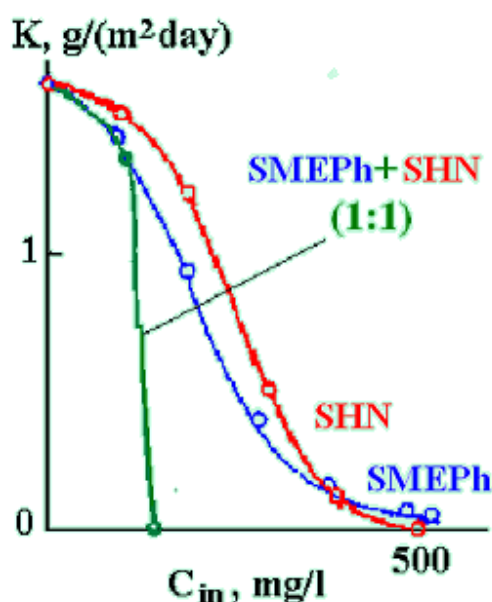


Figure 11. Dependence of the corrosion rate of a rotating cylinder made of steel St 3 on the content of SONP, SMEPh, and an equimolar mixture thereof.

In addition to development of mixtures, there is yet another method of increasing the protective action of CI nanolayers on metals. About ten years ago our ellipsometric and electrochemical studies have revealed that there are possibilities of improving the high carboxylate adsorption by preliminary modification of the metal surface by adsorption of another carboxylate. This was first observed when the adsorption of SMEPh begins at lower concentrations if SPhU has been pre-adsorbed on the oxidized iron electrode. This case was first considered in [4] and discussed in detail in Part I of our review [7]. It seems likely that the attractive interactions of SMEPh anions with already adsorbed SPhU are stronger than those of SMEPh with oxidized iron: formally, the calculated value of $(-\Delta G_a^0) = 38.4$ instead of 27.3 kJ/mol. Moreover, if after the adsorption of SMEPh anions in an amount corresponding to their monolayer, the SMEPh solution is substituted by pure borate buffer and then SPhU is introduced, the adsorption of the third nanolayer in the region of medium coverages is well described by Langmuir's equation. The calculated value of $(-\Delta G_a^0) = 39.2$ kJ/mol is significantly higher than that obtained for the first layer of SPhU adsorbed on oxidized iron, $(-\Delta G_a^0) = 33.1$ kJ/mol.

Thus, subsequent adsorption of the carboxylate anions on metals increases their $(-\Delta G_a^0)$ and, correspondingly, improves the protective properties of these nano-scale adsorption layers (their total thickness does not exceed 5 nm). It is significant that this method of sequential adsorption is possible from diluted solutions of individual CIs. After modification of metal surfaces by carboxylate chemisorption, adsorption not only of another carboxylate but also of a CI belonging to another class of organic compounds can be improved. This was illustrated above by adsorption of dimegin (modifier) and BTA on copper and mild steel.

Not only a CI of carboxylate type can be used as a modifier of metal surface. This area of research has been developed intensely in our lab in the past years. The results were already reported at EUROCORR-2010 and EUROCORR-2012. The success of later studies will be summarized in the following section of the present review.

Conclusions

1. Among the salts of monocarboxylic acids, sodium N-oleoylsarcozinate (SOS) is one of the best water-soluble organic nonoxidative passivators for steels, Cu, Zn, Mg, Al, and their alloys. SOS adsorption on metals from neutral aqueous solutions is often polymolecular in nature. The formation of the first monolayer of SOS started at very low C_{SOS} and was characterized by a high value of $(-\Delta G_a^0)$ indicating that the chemisorption of SOS is highly possible. The chemisorption layer together with the presence of hydrophobic tail group in SOS gives polymolecular film the ability to provide high protection for various metals in corrosive media.
2. Attempts to use various fatty acids to produce superhydrophobic coatings on metals, especially on copper, are worthy of notice. The nanolayers can provide contact angles $\Theta_c \geq 150^\circ$ and a low drop rolling angle of such surfaces. However, the superhydrophobic state is usually achieved by providing multimodal roughness to the surface. In order to obtain regularly ordered ridge-like or flower-like structures on the Cu surface, it was proposed to use ethanolic solutions not only of higher fatty acids but also their combination with others CIs or chemical compounds. Although some experiments could make the surface highly hydrophobic ($\Theta_c > 135^\circ$), attempts to achieve stable superhydrophobization of Cu in such a way failed so far.
3. Higher monocarboxylates and amino acids can be efficient CIs in a neutral environment for Al and its alloys. They can also be used for superhydrophobizing the surface after the anodization of pure Al (99.9%) or its alloy in combination with *N,N'*-dicyclohexylcarbodiimide. The most efficient CIs for Al alloys can be found among carboxylates which have a combination of the ability to form sparingly soluble compounds with Al^{3+} and cations of other metals the alloy contains, with high surface activity. For example, the passivating film formed for 10 min at $t = 60^\circ\text{C}$ in an aqueous solution containing 16 mM SOS twice more efficiently protects AMg6 alloy than the film formed in a similar chromate solution.
4. The passivation and especially the prevention of local depassivation of Fe and Cu are provided relatively easily by many carboxylates. However, efficient protection of Zn requires more hydrophobic carboxylates, e.g. even SA is an insufficiently efficient passivator for Zn. Higher amino acids may be more efficient CIs than fatty acids and their salts. A slight increase in the pH (from 7.4 to 9.1) can enhance the adsorption and the protective effect of amino carboxylates, for example SFPh. However, passivation of Zn even by efficient organic CIs such as SOS or SFPh, cannot provide long-term protection of the metal in corrosive media.

5. Salts of higher carboxylic acids and amino acids can also be used for passivation of Mg and its alloys. The protection effect of their salts is often related to the precipitation of an insoluble Mg salt, which mainly affects the anodic reaction. The aliphatic chain length controls the anion solubility and the reaction rate of Mg carboxylate formation. The higher alkylcarboxylic acids such as SA can provide good protection of Mg alloys. Since direct coating of Mg is not possible, it was proposed to subject the Mg (99.96%) to hydrothermal treatment at 120°C for 24 h to form an Mg(OH)₂ layer as the first step. After that, SA anchored on the Mg(OH)₂ sample grown by hydrothermal treatment, with formation of Mg stearate, which enhances bonding. SA coating enhances the corrosion resistance of Mg implants so that it could provide mechanical support in the initial period of bone healing. The high protective properties of Sol were revealed in the humid atmosphere with daily condensation of moisture on the samples of Mg where the appearance of the first corrosion damage was observed 6 times later than in the case of the passivation by the same concentration of chromates.
6. Since the admixture of iron in Mg alloy dissolves and forms cations in the solution, which are then reduced on its surface, corrosion is drastically accelerated. In order to prevent iron re-deposition, it was proposed to introduce an iron complexing agent into the corrosive aqueous solution. A correlation exists between the inhibiting efficiency and the values of complex stability constants, $K_{\text{sFe}^{\text{III}}}$, and sodium salicylate ($K_{\text{sFe}^{\text{III}}} = 36.8$) is one of the best CIs.
7. The vast majority of studies on the passivating ability of di- and polycarboxylates were previously performed on Fe and mild steels. No evidence of the advantages of these carboxylates was found in comparison with monocarboxylates as metal passivators in aqueous solutions. The reason for this is the poor adsorption on iron, although it can occur by two COO⁻ groups, and their insufficiently dense packing into the adsorption layer.
8. Although higher dicarboxylates were still insufficiently investigated as CIs of passivating type, recently a very efficient inhibitor, not only with respect to Fe but also to Cu, was found among them. Dimegin is the disodium salt of a protoporphyrin IX derivative belonging to the class of macrocyclic compounds. Its chemisorption on the metals from neutral aqueous solutions is beyond question, and it occurs both on reduced and oxidized surfaces of these metals.
9. New possibilities for improvement of the anticorrosive protection of metals are presented not only by using mixtures of some carboxylates but also by constructing multilayer nanocoating of various CIs from aqueous solutions. The metal surface is preliminarily modified by a solution of one carboxylate firmly adsorbing on it, and then adsorption of the second carboxylate or another CI is carried out.

Acknowledgements

This work was supported by the RFBR grant No. 16-03-00199 “Surface modification of Al, Mg and their alloys by nanolayers of organic corrosion inhibitors.”

References

1. Yu.I. Kuznetsov, *Organic Inhibitors of Corrosion of Metals*, 1996, New York, Plenum Press.
2. K. Schwabe, *Z. Phys. Chem.*, Leipzig, 1964, **226**, no. 1, 1.
3. I.L. Rozenfeld, Yu.I. Kuznetsov, I.Ya. Kerbeleva and V.P. Persiantseva, *Zashch. Met.*, 1975, **11**, no. 5, 612 (in Russian).
4. Yu.I. Kuznetsov and N.P. Andreeva, *Russ. J. Electrochem.*, 2006, **42**, no. 10, 1101.
5. Yu.I. Kuznetsov, *Prot. Met. Phys. Chem. Surf.*, 2011, **47**, no 7, 821.
6. A.A. Chirkunov, A.S. Gorbachev, Yu.I. Kuznetsov and N.P. Andreeva, *Prot. Met. Phys. Chem. Surf.*, 2013, **49**, no. 7, 854.
7. Yu.I. Kuznetsov, *Int. J. Corros. Scale Inhib.*, 2015, **4**, no. 4, 284. doi: [10.17675/2305-6894-2015-4-4-1](https://doi.org/10.17675/2305-6894-2015-4-4-1)
8. J.E.O. Mayne, *Proc. 4th European Symp. Corrosion Inhib.*, Ferrara, Italy, 1975, p. 1.
9. K. Takahashi, J.A. Bardwell, B. MacDougall and M.J. Graham, *Electrochim. Acta.*, 1992, **37**, 489.
10. U. Rammelt, S. Kohler and G. Reinhard, *Electrochim. Acta.*, 2008, **53**, 6968.
11. S. Turgoose, *Proc. 6th European Symp. Corrosion Inhib.*, Ferrara, Italy, 1985, 1041.
12. C. Hansch and A. Leo, *Correlation Analysis in Chemistry and Biology*, 1981, New York, J.Wiley.
13. L.P. Hammett, *Physical Organic Chemistry*, 1970, New York, McGraw-Hill Book Co.
14. Yu.I. Kuznetsov, in: *Reviews on Corrosion Inhibitor Science and Technology*, Eds. A. Raman and P. Labine, 1993, Houston, NACE, 1-3-1.
15. J.M. Godinez-Alvarez, J.L. Mora-Mendoza, E. Rodriguez-Betancourt, G. Zavala-Olivares and M.A. Gonzalez, in: *Reviews on Corrosion Inhibitor Science and Technology*, Eds. A. Raman, P. Labine and M.A. Quraishi, 2004, vol. 3, Houston, NACE International, 18-1.
16. Ya.G. Bober, Yu.I. Kuznetsov and N.P. Andreeva, *Russ. J. Electrochem.*, 2008, **44**, no. 1, 84.
17. Yu.I. Kuznetsov, M.O. Agafonkina, N.P. Andreeva and A.B. Solovyeva, *Prot. Met. Phys. Chem. Surf.*, 2010, **46**, no. 7, 743.
18. Yu.I. Kuznetsov, *Prot. Met. Phys. Chem. Surf.*, 2011, **47**, no. 7, 821.
19. U. Rammelt, S. Kohler and G. Reinhard, *Corros. Sci.*, 2011, **53**, 3515.
20. M.O. Agafonkina, Yu.I. Kuznetsov, N.P. Andreeva, Yu.E. Pronin and L.P. Kazansky, *Prot. Met. Phys. Chem. Surf.*, 2012, **48**, no. 7, 773.
21. N.P. Andreeva, Ya.G. Bober and Yu.I. Kuznetsov, *Korrozi.: mater., zashch.*, 2009, no. 9, 28 (in Russian).
22. A. Frignani, V. Grassi, F. Zanotto and F. Zucchi, *Corros. Sci.*, 2012, **63**, 29.
23. Nandini Dinodi and A.Nityananda Shetty, *Corros. Sci.*, 2014, **85**, 411.
24. N.P. Andreeva, Yu.V. Ushakova, Yu.I. Kuznetsov, M.O. Agafonkina, L.P. Kazansky and Yu.Ya. Andreev, *Prot. Met. Phys. Chem. Surf.*, 2014, **50**, no. 7, 860.
25. G. Žerjav and I. Milošev, *Int. J. Electrochem. Sci.*, 2014, no. 9, 2696.

26. M.O. Agafonkina, Yu.I. Kuznetsov, and N.P. Andreeva, *Russ. J. Phys. Chem.*, 2015, **89**, no. 6, 1013.
27. G. Žerjav and I. Milošev, *Corros. Sci.*, 2015, **98**, 180.
28. M.B. Petrovic Michjlovic and M.M. Antonijevic, *Int. J. Electrochem. Sci.*, 2015, **10**, 1027.
29. Yu.I. Kuznetsov, M.O. Agafonkina, N.P. Andreeva and L.P. Kazansky, *Corros. Sci.*, 2015, **100**, 535.
30. G. Ruba H. Florence, F. Noreen Anthony, J. Wilson Sahayaraj, A.J. Amalraj, and S. Rajendran, *Ind. J. Chem. Technol.*, 2005, **12**, 472.
31. R.A. Scherrer and S.M. Howard, *J. Med. Chem.*, 1977, **20**, 53.
32. H. Terada, S. Muraoka and T. Fujita, *J. Med. Chem.*, 1974, **17**, no. 3, 330.
33. J.A. Riddick, W.B. Bunger and T.K. Sakano, *Techniques of Chemistry, vol. II, Organic Solvents. 4th ed.*, New York, John Wiley and Sons, 1985, 379.
34. M. Tsunekawa, Zhang Zhi Yuan and T. Takamori, *Bull. Fac. Eng., Hokkaido Univ.*, 1988, no. 141, 27.
35. G.A. Salensky, M.G. Cobb and D.S. Everhart, *Ind. Eng. Chem. Prod. Res. Dev.*, 1986, **25**, no. 2, 133.
36. M.O. Agafonkina, A.M. Semiletov, Yu.I. Kuznetsov, N.P. Andreeva and A.A. Chirkunov, *Korroz.: mater., zashch.*, 2016, no. 5, 15 (in Russian).
37. A.M. Semiletov, Yu.I. Kuznetsov and A.A. Chirkunov, *Korroz.: mater., zashch.*, 2016, no. 6, 29 (in Russian).
38. A.M. Semiletov, Yu.I. Kuznetsov and A.A. Chirkunov, *Korroz.: mater., zashch.*, 2016, no. 7, 35 (in Russian).
39. *Chemical Encyclopedia (Bol'shaya Ross. Entsiklopediya)*, Moscow, 1995, **4**, p. 580 (in Russian).
40. R. Bordes, J. Tropsch, and K. Holmberg, *Langmuir*, 2010, **26**, 3077.
41. R. Bordes, J. Tropsch, and K. Holmberg, *Langmuir*, 2010, **26**, 10935.
42. N.P. Andreeva, M.O. Agafonkina, and Yu.I. Kuznetsov, *Korroz.: mater., zashch.*, 2010, no. 9, 7 (in Russian).
43. Yu.I. Kuznetsov and L.P. Kazansky, *Russ. Chem. Rev.*, 2008, **77**, no. 3, 219.
44. A.M. Emel'yanenko and L.B. Boinovich, *Russ. Chem. Rev.*, 2008, **77**, no. 7, 619.
45. S. Wang, L. Feng and L. Jiang, *Adv. Mater.*, 2006, **18**, 767.
46. R. Fushs-Godec and G. Zerjav, *Corros. Sci.*, 2015, **97**, 7.
47. K. Aramaki, *Corros. Sci.*, 2006, **48**, 3298.
48. K. Aramaki, *Corros. Sci.*, 2001, **43**, 2201.
49. C. Monticelli, G. Brunoro, A. Frignani and F. Zucchi, *Corros. Sci.*, 1991, **32**, 693.
50. I. Raspini, *Corrosion*, 1993, **49**, 821.
51. G. Bereket, A.S. Sarac and M. Kose, *Commun. Fac. Sci. Univ. Ank. Series B.*, 1996, **42**, 39.
52. A.A. El-Shafei, M.N.H. Moussa and A.A. El-Far, *J. Appl. Electrochem.*, 1997, **27**, 1075.

53. D. Daloz, C. Rapin, P. Steinmetz and G. Michot, *Corrosion*, 1998, **54**, 444.
54. G. Boisier, N. Portail and N. Pébère, *Electrochim. Acta*, 2010, **55**, 6182.
55. Yansheng Yin, Tao Liu, Shougang Chen, Tong Liu and Sha Cheng, *Appl. Surf. Sci.*, 2008, **255**, 2978.
56. Qi Wang, Bingwu Zhang, Mengnan Qu, Junyan Zhang and Deyan He, *Appl. Surf. Sci.*, 2008, **254**, 2009.
57. S.V. Lamaka, M.L. Zheludkevich, K.A. Yasakau, M.F. Montemor and M.G.S. Ferreira, *Electrochim. Acta*, 2007, **52**, 7231.
58. T.G. Harvey, S.G. Hardin, A.E. Hughes, T.H. Muster, P.A. White, T.A. Markley, P.A. Corrigan, J. Mardel, S.J. Garcia, J.M.C. Mol and A.M. Glenn, *Corros. Sci.*, 2011, **53**, 2184.
59. A. Balbo, A. Frignani, V. Grassi and F. Zucchi, *Corros. Sci.*, 2013, **73**, 80.
60. A. Frignani, A. Balbo, V. Grassi and F. Zucchi, *Int. J. Corros. Scale Inhib.*, 2013, **2**, no. 2, 138. doi: [10.17675/2305-6894-2013-2-2-138-149](https://doi.org/10.17675/2305-6894-2013-2-2-138-149)
61. Y. Liu, Z. Yu, S. Zhou and L. Wu, *Appl. Surf. Sci.*, 2006, **252**, 3818.
62. F. Zucchi, V. Grassi and F. Zanotto, *Mater. Corros.*, 2009, **60**, no. 3, 199.
63. A. Mesbah, C. Jyers, F. Lacouture, S. Mathieu, E. Rocca, M. François and J. Steinmetz, *Solid State Sci.*, 2007, **9**, 322.
64. W.F. Ng, M.H. Wong, F.T. Cheng, *Surf. Coat. Technol.*, 2010, **204**, 1823.
65. Q. Zhang, G.Q. Yie, Y. Li, Q.S. Yang and T. Nagai, *Int. J. Pharm.*, 2000, **200**, 153.
66. N.H. Helal, W.A. Badawy, *Electrochim. Acta*, 2011, **56**, 6581.
67. D. Höche, C. Blawert, S.V. Lamaka, N. Scharnagl, C. Mendis and M.L. Zheludkevich, *Phys. Chem. Chem. Phys.*, 2016, **18**, 1279.
68. S.V. Lomaka, D. Höche, R.P. Petrauskas, C. Blawert and M.L. Zheludkevich, *Electrochem. Commun.*, 2016, **62**, 5.
69. P. Hersch, J.B. Hare, A. Robertson and Sh.M. Sutherland, *J. Appl. Chem.*, 1961, **11**, 246.
70. N.R. Shmeleva, V.P. Barannik, *Zh. Prikl. Khim.*, 1963, **76**, 813 (in Russian).
71. J.I.O. Mayne and C.L. Page, *British Corros. J.*, 1972, **7**, no. 3, 111; 1974, **9**, no. 4, 223.
72. A.D. Mercer, *Proc. 5th European Symp. on Corrosion Inhib.*, Ferrara (Italy), 1980, **2**, 563.
73. K. Aramaki and T. Shimura, *Corros. Sci.*, 2004, **46**, 313.
74. M.O. Agafonkina, Yu.I. Kuznetsov, N.P. Andreeva and A.B. Solovyeva, *Korroz.: mater., zashch.*, 2013, no. 8, 19 (in Russian).
75. V.V. Feng, S. Chen, W. Guo, Y. Zhang and G. Liu, *J. Electroanal. Chem.*, 2007, **602**, 115.
76. N.P. Andreeva, M.O. Agafonkina and Yu.I. Kuznetsov, *Korroz.: mater., zashch.*, 2010, no. 9, 7 (in Russian).
77. I.L. Rozenfeld, *Corrosion Inhibitors*, New York: McGraw Hill Inc., 1981.
78. G.R.H. Florence, A.N. Anthony, J.W. Sahayaraj, A.J. Amalraj and S. Rajendran, *Ind. J. Chem. Technol.*, 2005, **12**, July, 472.

-
79. A. Chirkunov and Yu. Kuznetsov, *Corrosion Inhibitors in Cooling Water Systems*, in: Mineral Scales and Deposits: Scientific and Technological Approaches, eds. Z. Amjad and K.D. Demadis, Elsevier B.V., 2015, pp. 85–105.
 80. A.A. Chirkunov, I.A. Filippov, T.G. Murzabekova and O.V. Sorokina, *Korrozi.: mater., zashch.*, 2009, no. 3, 1 (in Russian).
 81. I.N. Putilova, S.A. Balezin and V.P. Barannik, *Corrosion Inhibitors of Metals*, 1958, Moscow, Goskhimizdat (in Russian).
 82. Yu.I. Kuznetsov, in: *Advances in Science and Technology. Series: Corrosion and Corrosion Protection*, vol. 7, 1978, Moscow, VINITI, pp. 159–205.
 83. L.I. Antropov, E.M. Makushin and V.F. Panasenko, *Inhibitors of Corrosion of Metals*, 1981, Technika, Kiev (in Russian).
 84. G. Trabanelli, in: *Reviews on Corrosion Inhibitor Science and Technology*, eds. A. Raman and P. Labine, 1993, NACE International, Houston, USA, I-2-1.
 85. Yu.I. Kuznetsov and N.P. Andreeva, in: *Reviews on Corrosion Inhibitor Science and Technology*, vol. 2, eds. A. Raman and P. Labine, 1996, NACE International, Houston, USA, I-1-17.
 86. Yu.I. Kuznetsov, Ya.G. Bober, N.P. Andreeva and L.P. Kazansky, *EUROCORR 2008*, 7-11 September 2008, Edinburgh, Fulltext 1223.pdf, pp. 1–10.
 87. Yu.I. Kuznetsov, *Prot. Met. Phys. Chem. Surf.*, 2015, **51**, no. 7, 1111.

